Photon correlation functions and photon blockade in two-mode cavity QED

Simon James Whalen

Supervisor: Professor Howard J. Carmichael

Bachelor of Science (Honours)
in
Physics

The University of Auckland
2008

Abstract

Cavity quantum electrodynamics (cavity QED) is the study of systems in which atoms interact with the mode or modes of an optical cavity. In this dissertation, we compute second-order photon correlation functions in a system where two optical cavity modes with orthogonal linear polarisations interact with an atom via an $F = 4 \longleftrightarrow F' = 5$ transition. We take into account the full atomic level structure for this transition, including the Zeeman energy shift. One cavity mode couples the $F = 4$ atomic state to the $F' = 5$ state via $\Delta m_F = 0$ transitions; the other cavity mode couples the atomic states via $\Delta m_F = \pm 1$ transitions. The former mode is driven by a coherent laser field.

We first consider second-order photon correlation functions obtained using an analytic treatment of the simple system comprising a two-level atom in a single-mode cavity, in the weak excitation regime. Then we move on to a more comprehensive treatment, including the full atomic level structure and two cavity modes, again in the weak excitation regime. For the more complicated system, we use numerical solutions of the master equation for the system density operator, allowing us to compute steady state photon correlation functions for a variety of parameters. In our results, we identify uniquely quantum phenomena.

Acknowledgements

I would like to acknowledge and thank my supervisor, Professor Howard Carmichael, whose help and guidance was invaluable during the course of this project.

Contents

List of Figures

Chapter 1

Introduction

1.1 Motivation

The complexity of a computational task relates to how the problem scales with size. Suppose the time taken to solve a problem increases as a polynomial function of the size of its input. Such a problem is said to belong to the *polynomial complexity class*, **P**. If, on the other hand, the time taken to solve a problem increases faster than a polynomial function, then the problem belongs to the *non-polynomial complexity class*, **NP**. Problems in the **NP** class pose difficulties to computer scientists, because of how rapidly the amount of computer time increases with the size of the problem. Such problems are in practice intractable using conventional computer hardware.

While the underlying physics of modern computer components is governed by quantum mechanics, the actual data encoded in the hardware is entirely classical. It was the problem of simulating quantum systems — a problem which gets exponentially more difficult to solve as the size of the system increases — which led Richard Feynman to suggest in 1982 that computers ought to be equipped with quantum hardware, so that the computer's computational power would scale at the same rate as the complexity of the system being simulated [11]. In 1985, David Deutsch outlined the basic principles of quantum computation, and proposed the idea of a *quantum computer*. Deutsch showed that such a computer could in theory solve problems that cannot be efficiently solved with a classical computer [9]. In 1994, Peter Shor showed that a quantum computer could be used to find the prime factors of a large integer in polynomial time [18]. Modern encryption algorithms, including the widely used RSA algorithm, rely on the fact that factoring large integers is very difficult with classical computers. Thus, quantum computing is of great importance and interest to cryptographers and other scientists.

Classical computers store data as binary bits, which take values of either 0 or 1. One important concept in quantum computing is the idea of a quantum bit, or *qubit*, which provides a quantum analogue to classical data. A qubit must have two orthogonal basis states, which we will call $|0\rangle$ and $|1\rangle$. Unlike a classical bit, a qubit can represent not only the pure states $|0\rangle$ and $|1\rangle$, but also a linear superposition of the two. The state of the qubit should furthermore be readily measurable.

One example of a qubit is a two-level atom, whose excitation state encodes the data. We define the $|0\rangle$ and $|1\rangle$ states to correspond to the ground and excited states of the atom respectively. The potential for use in quantum computing motivates the detailed study of two-level atoms, in particular atoms in optical cavities where the atoms may strongly interact with single photons. The system of a two-level atom coupled to a single cavity mode is known as the *Jaynes-Cummings model*; models of more complicated systems, with multi-level atoms, can be developed using its basic ideas.

In this dissertation we will study the non-classical properties of both simple Jaynes-Cummings systems, and of more complicated systems which include an additional cavity mode and more com-

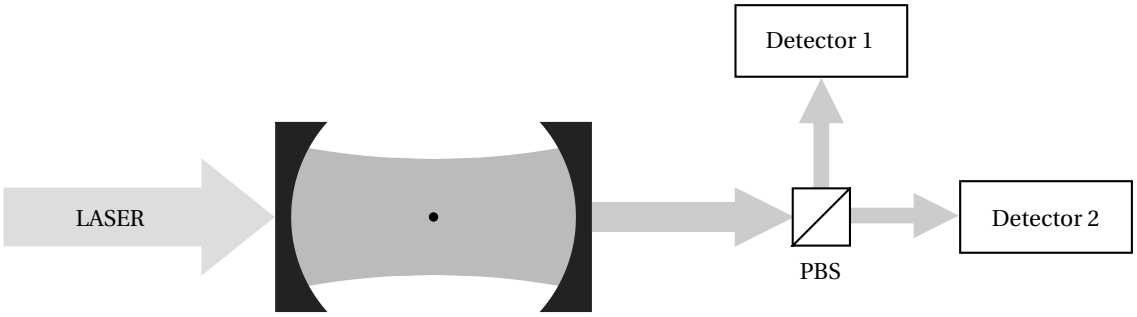

Figure 1.1: Schematic experimental setup. The abbreviation 'PBS' refers to a polarising beam splitter. The atom is localised in the centre of the cavity.

plicated atomic level structure. Knowledge of the behaviour of such systems may one day lead to applications in the field of quantum computing, or in related fields. Knowledge of how multi-level atoms behave in comparison with idealised two-level systems has direct relevance to whether or not such multi-level atoms can be used as qubits to encode quantum information.

1.2 Schematic experimental setup

In their 2005 paper [5], Birnbaum *et. al.* report observations of so-called *photon blockade* in the light transmitted by an optical cavity containing a single trapped Caesium atom strongly coupled to the cavity field. Photon blockade occurs when the absorption of an input photon by some optical device blocks the transmission of a second photon. This phenomenon converts an incoming poissonian stream of photons into a sub-poissonian stream which furthermore exhibits *photon antibunching*, where the photons in the stream exiting the apparatus come out with regular gaps between them.

Two optical cavity modes with orthogonal linear polarisations interact with the atom via the $6S_{1/2}, F = 4 \longleftrightarrow 6P_{3/2}, F' = 5$ hyperfine transition in Caesium, at 852.4 nm. An external magnetic field introduces a quantisation axis such that one cavity mode couples the $F = 4$ atomic ground state to the $F' = 5$ excited state via $\Delta m_F = 0$ transitions. This mode is driven by a coherent laser field. The other cavity mode with orthogonal polarisation to the driven mode couples the atomic states via $\Delta m_F = \pm 1$ transitions. A schematic diagram of the experimental setup is shown in Fig. 1.1.

Light escaping from the cavity by spontaneous emission of the atom leaks out through the sides of the cavity. Light leaking out through one of the cavity mirrors, on the other hand, is passed through a polarising beam splitter, so that the output from each cavity mode can be detected separately. The photon statistics for the light output from the cavity are used to characterise the behaviour of the system.

1.3 Photon correlation functions

1.3.1 The classical second-order intensity correlation function

In order to quantify the way the intensity $I(t)$ of a classical light beam fluctuates with time, it is helpful to introduce the second-order intensity correlation function, defined by

$$g^{(2)}(\tau) = \frac{\langle I(t)I(t+\tau)\rangle}{\langle I(t)\rangle\langle I(t+\tau)\rangle} \tag{1.1}$$

where $\langle\cdots\rangle$ denotes an average with respect to t. Writing the intensity as the sum of its mean and a fluctuation, $I(t) \equiv \langle I\rangle + \Delta I(t)$, it is clear that $g^{(2)}(0)$ satisfies the inequality

$$g^{(2)}(0) = \frac{\langle I^2\rangle}{\langle I\rangle^2} = 1 + \frac{\langle \Delta I(t)^2\rangle}{\langle I\rangle^2} \geq 1, \tag{1.2}$$

and furthermore it can be shown [13, §6.3] that $g^{(2)}(\tau)$ has a global maximum at $\tau = 0$.

Consider now light with a constant mean intensity, such that $\langle I(t)\rangle = \langle I(t+\tau)\rangle$. For sufficiently large τ, $I(t)$ and $I(t+\tau)$ are statistically independent, yielding the result:

$$\lim_{\tau\to\infty} g^{(2)}(\tau) = 1. \tag{1.3}$$

There exists a limiting case of note: perfectly coherent, monochromatic light with a constant intensity. For such light, the second-order correlation function satisfies $g^{(2)}(\tau) = 1$ for all τ. Classically, light with $g^{(2)}(\tau) < 1$ is not possible. However, such a result is in fact obtained when one considers the light beam to consist not of classical electromagnetic waves but of photons.

1.3.2 The second-order photon correlation function: photon bunching and antibunching

For quantum light, i.e. a stream of photons, the second-order photon correlation function is given by

$$g^{(2)}(\tau) = \frac{\langle :\hat{n}_1(t)\hat{n}_2(t+\tau):\rangle}{\langle \hat{n}_1(t)\rangle\langle \hat{n}_2(t+\tau)\rangle} = \frac{\langle \hat{a}_1^\dagger(t)\hat{a}_2^\dagger(t+\tau)\hat{a}_2(t+\tau)\hat{a}_1(t)\rangle}{\langle \hat{a}_1^\dagger(t)\hat{a}_1(t)\rangle\langle \hat{a}_2^\dagger(t+\tau)\hat{a}_2(t+\tau)\rangle} \tag{1.4}$$

where $\hat{n}_i$ is the occupation number operator of the light impinging on detector i where $i = 1,2$. The reason we must now explicitly distinguish between the two detectors is that once a photon has been detected by one detector it cannot be detected by the other. In the classical case, we can split a beam in two and send half to each detector, but we cannot split a photon in two; each photon goes to one detector or the other, and hence the detectors must be distinguished. In this case, $\langle\cdots\rangle$ denotes a quantum-mechanical expectation value, obtained by taking the trace of the product of the operator in question and the density operator for the light beam.

The $:\cdots:$ symbols denote *normal ordering*, where all photon annihilation operators are written to the right of the creation operators in the expansion of the photon occupation operators. This is a consequence of the photoelectric detection process, which relies on the absorption of light, or the annihilation of photons.

It is possible to classify light according to the properties of the correlation function. The classification is as follows:

- bunched light: $g^{(2)}(\tau) \leq g^{(2)}(0)$,
- coherent light: $g^{(2)}(\tau) = 1$,

- antibunched light: $g^{(2)}(\tau) > g^{(2)}(0)$.

Furthermore the photon statistics of the light can be classified as super-poissonian ($g^{(2)}(0) > 1$), poissonian ($g^{(2)}(0) = 1$), or sub-poissonian ($g^{(2)}(0) < 1$). The cases of bunched and coherent light have classical analogues, but there is no classical situation in which one can obtain $g^{(2)}(0) < 1$, nor in which one can obtain $g^{(2)}(\tau) > g^{(2)}(0)$. Sub-poissonian photon statistics and photon antibunching are hence both uniquely quantum phenomena.

Coherent light, as in the classical case, has $g^{(2)}(\tau) = 1$ for all τ. Coherent light has poissonian photon statistics, with random time intervals between the photons.

Bunched light, as the name suggests, consists of a stream of photons with the photons clumped together in bunches. This means that there is a higher probability of detecting two photons with a short interval between them than with a long interval. Thermal light satisfies this case.

In the case of antibunched light, the photons in the stream are more equally spaced than in the case of coherent light; photons in a stream of antibunched light do not have a random spacing. Antibunched light has no classical analogue. Furthermore, an antibunched stream of photons can also potentially exhibit sub-poissonian photon statistics. Sub-poissonian photon statistics and photon antibunching are both non-classical phenomena; they can potentially occur together, but each can occur in the absence of the other [16, §6.5].

Chapter 2

Derivation of the Hamiltonian

2.1 The Jaynes-Cummings model

The system of a two-level atom coupled to a single cavity mode, whether or not it is excited by incident light, is known as the *Jaynes-Cummings model* [14]. It will serve as a simple base on which to build the model we will use for numerical computation.

The Jaynes-Cummings Hamiltonian is given in broad outline by:

$$\hat{H} = \hat{H}_A + \hat{H}_F + \hat{H}_I \tag{2.1}$$

where $\hat{H}_A$ is the Hamiltonian of the free atom, $\hat{H}_F$ is the Hamiltonian of the radiation field, and $\hat{H}_I$ is the Hamiltonian for the interaction between the atom and the field.

2.1.1 The Hamiltonian of the atom

Consider an atom with n energy eigenstates $|E_n\rangle$ and energies E_n. The Hamiltonian of the atom can be written

$$\hat{H}_A = \sum_n E_n |E_n\rangle\langle E_n|. \tag{2.2}$$

However in the two-level approximation, neglecting any degeneracy of those levels, we consider only the specific transition that satisfies

$$E_2 - E_1 = \hbar\omega_A \tag{2.3}$$

where ω_A is the frequency of the atomic transition. We ignore all other atomic energy levels. This approximation is applicable when the frequency of the light coincides with one of the optical transitions of the atom.

For a two-level atom with ground state $|g\rangle$ and excited state $|e\rangle$, the atomic Hamiltonian $\hat{H}_A$ can be expressed

$$\hat{H}_A = E_g |g\rangle\langle g| + E_e |e\rangle\langle e|. \tag{2.4}$$

If we take the zero of energy to be half way between the energies of the ground and excited states, the atomic Hamiltonian is given by

$$\hat{H}_A = \frac{\hbar\omega_A}{2}\left(|e\rangle\langle e| - |g\rangle\langle g|\right). \tag{2.5}$$

Here it is convenient to introduce the atomic raising and lowering operators

$$\hat{\sigma}_+ \equiv |e\rangle\langle g| \quad \text{and} \quad \hat{\sigma}_- \equiv |g\rangle\langle e| \tag{2.6}$$

so that the atomic Hamiltonian can be written

$$\hat{H}_A = \frac{\hbar\omega_A}{2}\hat{\sigma}_z \tag{2.7}$$

where

$$\hat{\sigma}_z = [\hat{\sigma}_+, \hat{\sigma}_-] = |e\rangle\langle e| - |g\rangle\langle g|. \tag{2.8}$$

2.1.2 The Hamiltonian of the radiation field

The Hamiltonian of the radiation field is given by [16, §4.4]

$$\hat{H}_F = \sum_{\mathbf{k}}\sum_{\lambda} \hbar\omega_k \left(\hat{n}_{\mathbf{k}\lambda} + \frac{1}{2}\right) = \sum_{\mathbf{k}}\sum_{\lambda} \hbar\omega_k \left(\hat{a}^\dagger_{\mathbf{k}\lambda}\hat{a}_{\mathbf{k}\lambda} + \frac{1}{2}\right) \tag{2.9}$$

where $\hat{n}_{\mathbf{k}\lambda}$ is the occupation number operator of the cavity mode specified by the wavevector $\mathbf{k}$ and the polarisation state λ.

The term

$$\sum_{\mathbf{k}}\sum_{\lambda} \frac{1}{2}\hbar\omega_k \tag{2.10}$$

is due to the *zero-point energy*, an infinite constant, and does not contribute to the energy of the electromagnetic field as determined by measurements of the intensity of a beam of light. Therefore we choose the zero of energy to be the zero-point energy; the Hamiltonian of the radiation field is consequently given by

$$\hat{H}_F = \sum_{\mathbf{k}}\sum_{\lambda} \hbar\omega_k \hat{a}^\dagger_{\mathbf{k}\lambda}\hat{a}_{\mathbf{k}\lambda}. \tag{2.11}$$

In the Jaynes-Cummings model, only a single cavity mode is considered. However it is useful to retain the more general expression, as later we will consider a system with two orthogonal cavity modes.

2.1.3 Atom-light interactions

The operator for the electric field expanded in travelling waves is given by

$$\hat{\mathbf{E}}_T(\mathbf{r}) = \mathrm{i}\sum_{\mathbf{k}}\sum_{\lambda} \mathbf{e}_{\mathbf{k}\lambda}\sqrt{\frac{\hbar\omega_k}{2\epsilon_0 V}}\left\{\hat{a}_{\mathbf{k}\lambda}e^{\mathrm{i}\mathbf{k}\cdot\mathbf{r}} - \hat{a}^\dagger_{\mathbf{k}\lambda}e^{-\mathrm{i}\mathbf{k}\cdot\mathbf{r}}\right\} \tag{2.12}$$

where $V = L^3$ is the volume of the cavity, $\mathbf{e}_{\mathbf{k}\lambda}$ is a unit polarisation vector (taken to be real for linearly polarised light), and the other symbols have their usual meanings. The field inside a cavity looks similar, but the mode functions $e^{\pm\mathrm{i}\mathbf{k}\cdot\mathbf{r}}$ are replaced with functions that depend on the particular shape of the cavity considered.

It is usually the case in quantum optics that the wavelength of the electromagnetic field interacting with the atom (on the order of several hundred nanometres for visible light) is much greater than the size of the atom itself (on the order of the Bohr radius, ~ 0.5 Å). Thus it is possible to evaluate the electromagnetic field at the position of the atom $\mathbf{r}_A$. Later on, this will enable us to absorb the mode functions in Eq. (2.12) into a phase regardless of the particular geometry of the cavity.

It is also sufficient to approximate the interaction energy between the atom and the electromagnetic field by the electric-dipole interaction energy. The electric-quadrupole and magnetic-dipole contributions are smaller than the electric-dipole contribution by a factor on the order of the fine structure constant, $\alpha \approx 1/137$, so they can be neglected except in the case of very strong fields.

The resulting electric-dipole interaction Hamiltonian is

$$\hat{H}_I = -\hat{\mathbf{d}} \cdot \hat{\mathbf{E}}_T \tag{2.13}$$

with

$$\hat{\mathbf{d}} = -e\hat{\mathbf{D}} = -e\sum_{n=1}^{Z} \hat{\mathbf{r}}_n \tag{2.14}$$

where n runs over Z electrons with charge $-e$.

Note that $\hat{\mathbf{D}}$ can be written in the form

$$\hat{\mathbf{D}} = \sum_i |i\rangle\langle i|\hat{\mathbf{D}}\sum_j |j\rangle\langle j| = \sum_{i,j} \mathbf{D}_{ij}|i\rangle\langle j| \tag{2.15}$$

using closure relations for the atomic energy eigenstates $|i\rangle$ and $|j\rangle$, where

$$\mathbf{D}_{ij} = \langle i|\hat{\mathbf{D}}|j\rangle. \tag{2.16}$$

Note also that when $i = j$, $\mathbf{D}_{ij} = 0$, because $\hat{\mathbf{D}}$ is an odd-parity operator. Therefore we obtain for the interaction Hamiltonian

$$\hat{H}_I = \mathrm{i}e\sum_{\mathbf{k}}\sum_{\lambda}\sum_{i,j}\sqrt{\frac{\hbar\omega_k}{2\epsilon_0 V}}\mathbf{e}_{\mathbf{k}\lambda}\cdot\mathbf{D}_{ij}\left\{\hat{a}_{\mathbf{k}\lambda}e^{\mathrm{i}\mathbf{k}\cdot\mathbf{r}_A} - \hat{a}^\dagger_{\mathbf{k}\lambda}e^{-\mathrm{i}\mathbf{k}\cdot\mathbf{r}_A}\right\}|i\rangle\langle j|. \tag{2.17}$$

In an effectively two-level atom, the sum over i, j only runs over two states, $|g\rangle$ and $|e\rangle$. Consider the wavefunctions for the states $|g\rangle$ and $|e\rangle$, which we will write as $\psi_g(x)$ and $\psi_e(x)$ respectively. The matrix elements of $\hat{\mathbf{D}}$ can be written in terms of these wavefunctions as follows:

$$\langle g|\hat{\mathbf{D}}|e\rangle = \int dx' \int dx''\langle g|x'\rangle\langle x'|\hat{\mathbf{D}}|x''\rangle\langle x''|e\rangle = \int dx' \int dx''\psi^*_g(x')\langle x'|\hat{\mathbf{D}}|x''\rangle\psi_e(x''), \tag{2.18a}$$

$$\langle e|\hat{\mathbf{D}}|g\rangle = \int dx' \int dx''\langle e|x'\rangle\langle x'|\hat{\mathbf{D}}|x''\rangle\langle x''|e\rangle = \int dx' \int dx''\psi^*_e(x')\langle x'|\hat{\mathbf{D}}|x''\rangle\psi_g(x''). \tag{2.18b}$$

$\hat{\mathbf{D}}$ is a function of the position operator x so we have the relation [17, §1.7]

$$\langle x'|\hat{\mathbf{D}}|x''\rangle = \hat{\mathbf{D}}\delta\left(x' - x''\right), \tag{2.19}$$

which allows us to write the double integral in each of Eqs. (2.18) as a single integral:

$$\langle g|\hat{\mathbf{D}}|e\rangle = \int dx'\psi^*_g(x')\hat{\mathbf{D}}\psi_e(x'), \tag{2.20a}$$

$$\langle e|\hat{\mathbf{D}}|g\rangle = \int dx'\psi^*_e(x')\hat{\mathbf{D}}\psi_g(x'). \tag{2.20b}$$

If the wavefunctions $\psi_g(x)$ and $\psi_e(x)$ are assumed to be real, we find that the matrix elements $\mathbf{D}_{ge}$ and $\mathbf{D}_{eg}$ are equal real vectors. Therefore we obtain

$$\hat{H}_I = \hbar\sum_{\mathbf{k}}\sum_{\lambda}\left\{g_{\mathbf{k}\lambda}\hat{a}_{\mathbf{k}\lambda} + g^*_{\mathbf{k}\lambda}\hat{a}^\dagger_{\mathbf{k}\lambda}\right\}(\hat{\sigma}_+ + \hat{\sigma}_-) \tag{2.21}$$

where we have used the atomic raising and lowering operators from Eq. (2.6), and where we have defined the *coupling constant* $g_{\mathbf{k}\lambda}$, given by

$$g_{\mathbf{k}\lambda} = \mathrm{i}e\sqrt{\frac{\omega_k}{2\epsilon_0\hbar V}}\mathbf{e}_{\mathbf{k}\lambda}\cdot\mathbf{D}_{ge}e^{\mathrm{i}\mathbf{k}\cdot\mathbf{r}_A}. \tag{2.22}$$

This interaction Hamiltonian, when expanded out, contains terms in $\hat{a}\hat{\sigma}_+$ and $\hat{a}^\dagger\hat{\sigma}_-$, which conserve energy, as well as terms in $\hat{a}\hat{\sigma}_-$ and $\hat{a}^\dagger\hat{\sigma}_+$ which do not conserve energy to first order (but do conserve energy if two-photon or multiple-photon processes are taken into account). We neglect those terms which do not conserve energy to first order, making the *rotating-wave approximation*. This yields an interaction Hamiltonian

$$\hat{H}_I = \hbar \sum_{\mathbf{k}} \sum_{\lambda} \left\{ g_{\mathbf{k}\lambda} \hat{a}_{\mathbf{k}\lambda} \hat{\sigma}_+ + g^*_{\mathbf{k}\lambda} \hat{a}^\dagger_{\mathbf{k}\lambda} \hat{\sigma}_- \right\}. \tag{2.23}$$

It is convenient to absorb the complex phase of the coupling constant into the definitions of the atomic operators by making the transformations

$$g_{\mathbf{k}\lambda} \rightarrow -\mathrm{i} g_{\mathbf{k}\lambda} e^{-\mathrm{i}\phi} \tag{2.24a}$$
$$\hat{\sigma}_+ \rightarrow e^{\mathrm{i}\phi} \hat{\sigma}_+ \tag{2.24b}$$
$$\hat{\sigma}_- \rightarrow e^{-\mathrm{i}\phi} \hat{\sigma}_- \tag{2.24c}$$

which yield the final interaction Hamiltonian

$$\hat{H}_I = -\mathrm{i}\hbar \sum_{\mathbf{k}} \sum_{\lambda} g_{\mathbf{k}\lambda} \left\{ \hat{a}_{\mathbf{k}\lambda} \hat{\sigma}_+ - \hat{a}^\dagger_{\mathbf{k}\lambda} \hat{\sigma}_- \right\}. \tag{2.25}$$

2.1.4 The Jaynes-Cummings Hamiltonian

Substituting (2.7), (2.11), and (2.25) into Eq. (2.1), and considering only one mode of the field, we obtain the full Jaynes-Cummings Hamiltonian for a two-level atom coupled to a single cavity mode with dipole coupling constant g. The Jaynes-Cummings Hamiltonian is given by

$$\hat{H} = \frac{\hbar\omega_A}{2} \hat{\sigma}_z + \hbar\omega_L \hat{a}^\dagger \hat{a} - \mathrm{i}\hbar g \left(\hat{a}\hat{\sigma}_+ - \hat{a}^\dagger \hat{\sigma}_- \right) \tag{2.26}$$

where $\hbar\omega_A$ is the difference between the energies of the atomic ground and excited states and ω_L is the frequency of the incident light.

2.2 Extensions to the model

Now we go about implementing some extensions to the Jaynes-Cummings model of the atom to better model our specific atom-cavity system.

2.2.1 Cavity-laser interactions

The Hamiltonian for a coherently driven cavity (containing no atom) is

$$\hat{H} = \hat{H}_F + \hat{H}_{LC} \tag{2.27}$$

where $\hat{H}_F$ is the free Hamiltonian for the quantised cavity mode given by

$$\hat{H}_F = \hbar\omega_a \hat{a}^\dagger \hat{a} \tag{2.28}$$

and $\hat{H}_{LC}$ is the interaction between the cavity and a classical laser field. In the case where the laser frequency ω_L is close to resonance with a cavity mode a of frequency ω_a, the laser-cavity interaction is given by [15, §1.3.4]

$$\hat{H}_{LC} = \varepsilon \frac{\mathrm{i}c\mathscr{E}_0}{2\omega_L} \mathbf{e} \left\{ e^{-\mathrm{i}(\omega_L t + \phi_0)} - e^{\mathrm{i}(\omega_L t + \phi_0)} \right\} \cdot \sqrt{\frac{2\pi\hbar c^2}{\omega_a V}} \mathbf{e} \left\{ e^{\mathrm{i}\varphi_0} \hat{a} + e^{-\mathrm{i}\varphi_0} \hat{a}^\dagger \right\} \tag{2.29}$$

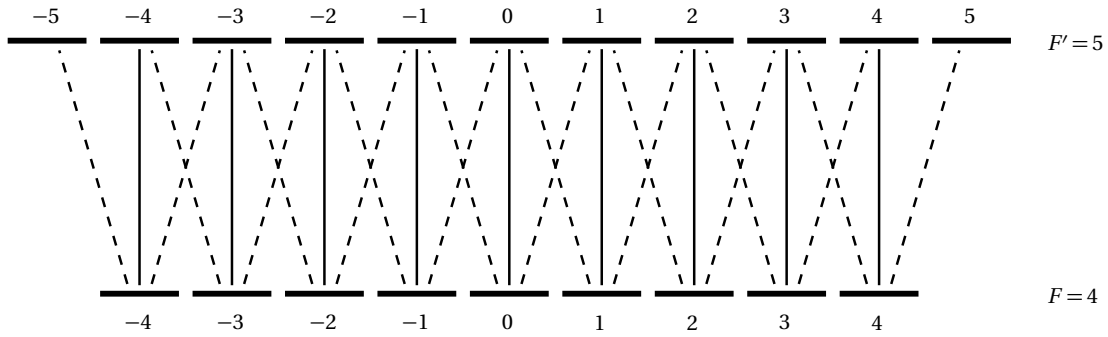

Figure 2.1: Atomic level structure and electric-dipole allowed transitions for an $F = 4 \longleftrightarrow F' = 5$ transition. The relative transition strengths are determined by appropriate Clebsch-Gordan coefficients. The driven cavity mode interacts with the atom via $\Delta m_F = 0$ transitions, and the non-driven mode via $\Delta m_F = \pm 1$ transitions.

where ε is a coupling constant between the laser field and the driven cavity mode. The laser field has amplitude $\mathscr{E}_0$, phase φ_0, and polarisation $\mathbf{e}$. The polarisation is matched to that of the cavity mode considered.

Applying the rotating-wave approximation (in an interaction picture where $\tilde{a} = \hat{a}e^{-i\omega_L t}$), and using the fact that $\mathbf{e}\cdot\mathbf{e} = 1$, this simplifies to

$$\hat{H}_{LC} = i\hbar\mathscr{E}\left(\hat{a}^\dagger e^{-i\omega_L t} - \hat{a}e^{i\omega_L t}\right) \tag{2.30}$$

where the arbitrary phase $\phi_0 - \varphi_0$ has been absorbed into the definitions of the ladder operators, and we have defined

$$\mathscr{E} = \varepsilon\frac{c\mathscr{E}_0}{2\omega_L}\sqrt{\frac{2\pi c^2}{\hbar\omega_a V}}. \tag{2.31}$$

2.2.2 Two-mode cavity system

The system we are considering has not one but two cavity modes with orthogonal linear polarisations which interact with the atom. One cavity mode a is driven by a coherent laser field. The other cavity mode b is not. Using the results derived so far, we now present the Hamiltonian of a driven single-atom two-mode cavity system with a non-degenerate two-level atom, in which the atom couples to both cavity modes a and b with respective dipole coupling constants g_a and g_b:

$$\hat{H} = \frac{\hbar\omega_A}{2}\hat{\sigma}_z + \hbar\omega_a\hat{a}^\dagger\hat{a} + \hbar\omega_b\hat{b}^\dagger\hat{b} - i\hbar g_a\left(\hat{a}\hat{\sigma}_+ - \hat{a}^\dagger\hat{\sigma}_-\right) - i\hbar g_b\left(\hat{b}\hat{\sigma}_+ - \hat{b}^\dagger\hat{\sigma}_-\right) + i\hbar\mathscr{E}\left(\hat{a}^\dagger e^{-i\omega_L t} - \hat{a}e^{i\omega_L t}\right). \tag{2.32}$$

2.3 The Zeeman Effect

So far our derivations have been restricted to a two-level atom, neglecting any possible degeneracies of those levels. However as was stated earlier we are considering the $6S_{1/2}, F = 4 \longleftrightarrow 6P_{3/2}, F' = 5$ hyperfine transition in Caesium, and as such the two atomic energy levels contain degenerate sub-levels, depicted schematically in Fig. 2.1. In the presence of an external magnetic field, as is the case here, the degeneracy is lifted and the atomic levels are split into magnetic sublevels in accordance with the theory of the Zeeman effect.

2.3.1 Selection rules

According to Fermi's golden rule, the probability per unit time for a transition from an initial state $|\phi_i\rangle$ with energy E_i to a final state $|\phi_f\rangle$ with energy E_f, due to a perturbation W, is

$$\dot{P}_{i\to f} = \frac{2\pi}{\hbar}|\langle\phi_f|W|\phi_i\rangle|^2\delta\left(E_f - E_i\right) \tag{2.33}$$

where this expression is integrated over a continuum of states with $\int dE_f \rho\left(E_f\right)$. Therefore it is clear that the electric-dipole interaction $\hat{H}_I$ as defined in Section 2.1.3 induces no transition between states $|\phi_i\rangle$ and $|\phi_f\rangle$ if the matrix element $\langle\phi_f|\hat{H}_I|\phi_i\rangle$ vanishes. Transitions with vanishing matrix element are termed forbidden in the electric-dipole interaction, but may occur due to another interaction (the magnetic-dipole or electric-quadrupole interaction, for example). Investigation of these matrix elements therefore yields the selection rules for electric-dipole transitions.

The *Wigner-Eckart Theorem* (for which a proof is available in [17]) states that the matrix elements of a spherical tensor operator $T_q^{(k)}$ (of rank k with $2k+1$ elements $\{q\}$) with respect to angular-momentum eigenstates satisfy

$$\langle j', m'|T_q^{(k)}|j, m\rangle = \langle j', m'|j, m; k, q\rangle\langle j'||T^{(k)}||j\rangle, \tag{2.34}$$

where the double-bar matrix element $\langle j'||T^{(k)}||j\rangle$ is independent of m, m', and q. The first factor on the right-hand side of Eq. (2.34), $\langle j', m'|j, m; k, q\rangle$ is a Clebsch-Gordan coefficient for adding j and k to get j'.

A vector is a spherical tensor of rank one. Thus in the case of the electric-dipole operator $\hat{\mathbf{d}}$, we have $k = 1$ in Eq. (2.34). When we include the spin of the atomic nucleus together with the orbital and spin angular momentum of the electrons, the angular momentum eigenstates are labelled with the quantum numbers F, and the Wigner-Eckart theorem reads:

$$\langle F', m'_F|\hat{\mathrm{d}}_q|F, m_F\rangle = \langle F', m'_F|F, m_F; 1, q\rangle\langle F'||\hat{\mathbf{d}}||F\rangle, \tag{2.35}$$

with $q = -1, 0, 1$.

For hyperfine transitions where the Clebsch-Gordan coefficients in Eq. (2.35) do not vanish, the matrix element $\langle\phi_f|\hat{H}_I|\phi_i\rangle$ mentioned above is also non-vanishing, and the transition is dipole-allowed. Thus the Clebsch-Gordan coefficients provide us with selection rules for the hyperfine structure, which are similar [15, §1.3.3] to those for the fine structure (see, for example, [12, §5.3]). The selection rules for the hyperfine structure are:

$$\Delta F = 0, \pm 1 \tag{2.36a}$$

$$\Delta m_F = 0, \pm 1 \tag{2.36b}$$

are allowed transitions, but

$$F = 0 \nleftrightarrow F' = 0 \tag{2.36c}$$

$$m_F = 0 \nleftrightarrow m'_F = 0 \quad \text{if} \quad \Delta F = 0 \tag{2.36d}$$

are forbidden transitions.

2.3.2 Two-level atom with Zeeman substructure

In the system we are considering, an external magnetic field introduces a quantisation axis such that the driven cavity mode a couples the atomic ground state to the excited state via $\Delta m_F = 0$ transitions.

The other cavity mode b with orthogonal polarisation to the driven mode couples the atomic states via $\Delta m_F = \pm 1$ transitions.

For the time being we will consider the quantisation axis to be imposed by an external magnetic field with negligible Zeeman effect. Stronger magnetic fields, for which the energy level splitting due to the Zeeman effect will need to be taken into account, will be considered later.

To take into account the more complicated level structure, the Hamiltonian for the full two-mode cavity system in Eq. (2.32) will need to be modified by replacing the atomic raising and lowering operators $\hat{\sigma}_+$ and $\hat{\sigma}_-$ (defined in Eq. (2.6)) with modified raising and lowering operators $\Sigma^\dagger_{0,\pm1}$ and $\Sigma_{0,\pm1}$. The Hamiltonian for the full interaction between the atom and the two cavity modes was previously given by

$$\hat{H}_I = -\mathrm{i}\hbar g_a \left(\hat{a}\hat{\sigma}_+ - \hat{a}^\dagger \hat{\sigma}_-\right) - \mathrm{i}\hbar g_b \left(\hat{b}\hat{\sigma}_+ - \hat{b}^\dagger \hat{\sigma}_-\right). \tag{2.37}$$

The new interaction Hamiltonian will be given by

$$\hat{H}_I = -\mathrm{i}\hbar g \left(\hat{a}\hat{\Sigma}^\dagger_0 - \hat{a}^\dagger \hat{\Sigma}_0\right) - \mathrm{i}\hbar g \left(\hat{b}\left[\frac{\hat{\Sigma}^\dagger_{-1} + \hat{\Sigma}^\dagger_{+1}}{\sqrt{2}}\right] - \hat{b}^\dagger \left[\frac{\hat{\Sigma}_{-1} + \hat{\Sigma}_{+1}}{\sqrt{2}}\right]\right) \tag{2.38}$$

where g is the maximum dipole coupling strength of the atomic $F = F_g \longleftrightarrow F' = F_e$ transitions, and where the new atomic raising and lowering operators (the so-called atomic dipole transition operators) have expansions in terms of atomic states and Clebsch-Gordan coefficients. In particular, the atomic lowering operators will be given by

$$\hat{\Sigma}_p = \sum_{m_{F,g}=-F_g}^{+F_g} C\left(F_e, m_{F,g}+p; F_g, m_{F,g}\right) |F_g, m_{F,g}\rangle\langle F_e, m_{F,g}+p| \tag{2.39}$$

with the Clebsch-Gordan coefficients defined by

$$C\left(F_e, m_{F,e}; F_g, m_{F,g}\right) \equiv \langle F_g, m_{F,g}; 1, m_{F,e} - m_{F,g} | F_e, m_{F,e}\rangle. \tag{2.40}$$

The matrix elements of the dipole operator are thus seen to be equal to the Clebsch-Gordan coefficients for adding spin 1 to spin $F_g = 4$ to reach total spin $F_e = 5$, given by (using the normal textbook notation) $\langle F_1 = 4, m_1; F_2 = 1, m_2 = -1, 0, +1 | F = 5, m = m_1 + m_2\rangle$. In the particular case where $F = F_1 + F_2$ and $m = m_1 + m_2$, the Clebsch-Gordan coefficients are given by [10]:

$$\langle F_1, m_1; F_2, m_2 | F = F_1 + F_2, m = m_1 + m_2\rangle = \left[\frac{(2F_1)!(2F_2)!(F_1+F_2+m_1+m_2)!(F_1+F_2-m_1-m_2)!}{(2F_1+2F_2)!(F_1-m_1)!(F_1+m_1)!(F_2-m_2)!(F_2+m_2)!}\right]^{\frac{1}{2}}. \tag{2.41}$$

In the cavity QED experiment we are modelling, the atomic transition is an $F = 4$ to $F' = 5$ transition. In this case the atomic lowering operators are given by:

$$\begin{aligned}\hat{\Sigma}_{-1} = {} & |g_{-4}\rangle\langle e_{-5}| + \sqrt{\frac{4}{5}}|g_{-3}\rangle\langle e_{-4}| + \sqrt{\frac{28}{45}}|g_{-2}\rangle\langle e_{-3}| + \sqrt{\frac{7}{15}}|g_{-1}\rangle\langle e_{-2}| + \sqrt{\frac{1}{3}}|g_0\rangle\langle e_{-1}| \\ & + \sqrt{\frac{2}{9}}|g_{+1}\rangle\langle e_0| + \sqrt{\frac{2}{15}}|g_{+2}\rangle\langle e_{+1}| + \sqrt{\frac{1}{15}}|g_{+3}\rangle\langle e_{+2}| + \sqrt{\frac{1}{45}}|g_{+4}\rangle\langle e_{+3}|, \end{aligned} \tag{2.42a}$$

$$\begin{aligned}\hat{\Sigma}_0 = {} & \sqrt{\frac{1}{5}}|g_{-4}\rangle\langle e_{-4}| + \sqrt{\frac{16}{45}}|g_{-3}\rangle\langle e_{-3}| + \sqrt{\frac{7}{15}}|g_{-2}\rangle\langle e_{-2}| + \sqrt{\frac{8}{15}}|g_{-1}\rangle\langle e_{-1}| + \sqrt{\frac{5}{9}}|g_0\rangle\langle e_0| \\ & \sqrt{\frac{8}{15}}|g_{+1}\rangle\langle e_{+1}| + \sqrt{\frac{7}{15}}|g_{+2}\rangle\langle e_{+2}| + \sqrt{\frac{16}{45}}|g_{+3}\rangle\langle e_{+3}| + \sqrt{\frac{1}{5}}|g_{+4}\rangle\langle e_{+4}|, \end{aligned} \tag{2.42b}$$

$$\hat{\Sigma}_{+1} = \sqrt{\frac{1}{45}}|g_{-4}\rangle\langle e_{-3}| + \sqrt{\frac{1}{15}}|g_{-3}\rangle\langle e_{-2}| + \sqrt{\frac{2}{15}}|g_{-2}\rangle\langle e_{-1}| + \sqrt{\frac{2}{9}}|g_{-1}\rangle\langle e_{0}| + \sqrt{\frac{1}{3}}|g_{0}\rangle\langle e_{+1}| \\ \sqrt{\frac{7}{15}}|g_{+1}\rangle\langle e_{+2}| + \sqrt{\frac{28}{45}}|g_{+2}\rangle\langle e_{+3}| + \sqrt{\frac{4}{5}}|g_{+3}\rangle\langle e_{+4}| + |g_{+4}\rangle\langle e_{+5}|. \quad (2.42c)$$

The raising operators can of course be found by taking the Hermitian adjoint of the lowering operators.

2.3.3 The Zeeman energy shift

The interaction energy between the electrons in the atom and and nuclear spin **I** gives rise to the hyperfine structure, with interaction energy

$$\hat{H}_{\text{HFS}} = A(J)\mathbf{I}\cdot\mathbf{J} \quad (2.43)$$

where $\mathbf{J} = \mathbf{L} + \mathbf{S}$ is the resultant of the total orbital and spin momenta of the electrons, and $A(J)$ is the hyperfine structure constant.

The interaction energy of the magnetic moment $\boldsymbol{\mu}$ of the atom with the applied magnetic field **B** is given by:

$$\hat{H}_{\text{mag}} = -\boldsymbol{\mu}\cdot\mathbf{B}. \quad (2.44)$$

We will be considering the Zeeman effect of a weak field, where $\hat{H}_{\text{mag}} \ll \hat{H}_{\text{HFS}}$.

The atomic magnetic moment is given by [12, §6.3]

$$\boldsymbol{\mu} = \boldsymbol{\mu}_J + \boldsymbol{\mu}_I = -g_J\frac{\mu_B}{\hbar}\mathbf{J} + g_I\frac{\mu_N}{\hbar}\mathbf{I} \quad (2.45)$$

where g_J is the Landé g-factor, g_I is the nuclear g-factor, and μ_B and μ_N are the Bohr and nuclear magnetons respectively. However $\mu_N \ll \mu_B$ so we can neglect the nuclear contribution, yielding

$$\hat{H}_{\text{mag}} = g_J\frac{\mu_B}{\hbar}\mathbf{J}\cdot\mathbf{B}. \quad (2.46)$$

When the interaction with the external magnetic field is weaker than the hyperfine interaction, as is the case here, then the vectors **J** and **I** move rapidly around their resultant **F**, while **F** precesses more slowly around the magnetic field. In this regime F and m_F are good quantum numbers, while m_J and m_I are not [12]. Thus the unperturbed eigenstates are the simultaneous eigenstates of $\mathbf{F}^2$, $\mathbf{J}^2$, $\mathbf{I}^2$ and F_z, which are $|FJIm_F\rangle$, and we need to take the projection of the magnetic moment along **F**:

$$\hat{H}_{\text{mag}} = g_J\frac{\mu_B}{\hbar}\frac{\langle\mathbf{J}\cdot\mathbf{F}\rangle}{F(F+1)}\mathbf{F}\cdot\mathbf{B} = g_F\frac{\mu_B}{\hbar}\mathbf{F}\cdot\mathbf{B} \quad (2.47)$$

where

$$g_F \approx g_J\frac{F(F+1)+J(J+1)-I(I+1)}{2F(F+1)} \quad (2.48)$$

with the Landé g-factor given by

$$g_J = 1 + \frac{J(J+1)+S(S+1)-L(L+1)}{2J(J+1)}. \quad (2.49)$$

Choosing the magnetic field to be applied along the z-axis, $\mathbf{B} = B\hat{\mathbf{z}}$, we obtain the interaction energy

$$\hat{H}_{\text{mag}} = g_F\frac{\mu_B}{\hbar}BF_z. \quad (2.50)$$

The Zeeman energy shift is therefore given by:

$$\begin{aligned}\Delta E &= \langle FJIm_F|\hat{H}_{\text{mag}}|FJIm_F\rangle \\ &= \langle FJIm_F|g_F\frac{\mu_B}{\hbar}BF_z|FJIm_F\rangle \\ &= g_F\mu_B m_F B,\end{aligned} \tag{2.51}$$

because of the fact that $F_z|FJIm_F\rangle = \hbar m_F|FJIm_F\rangle$.

Now we are in a position to modify the Hamiltonian of the free atom, originally given in Eq. (2.4). It now becomes

$$\hat{H}_A = \sum_{m_F=-4}^{4} E_{g,m_F}|g,m_F\rangle\langle g,m_F| + \sum_{m_F=-5}^{5} E_{e,m_F}|e,m_F\rangle\langle e,m_F| \tag{2.52}$$

with

$$E_{g,m_F} = E_{g,0} + g_{F,g}\mu_B m_F B \tag{2.53a}$$

$$E_{e,m_F} = E_{e,0} + g_{F,e}\mu_B m_F B \tag{2.53b}$$

where $g_{F,g}$ and $g_{F,e}$ are the different g-factors for the ground and excited states respectively. Note also that

$$E_{g,0} = -\frac{\hbar\omega_A}{2} \quad \text{and} \quad E_{e,0} = +\frac{\hbar\omega_A}{2}. \tag{2.54}$$

2.4 The system Hamiltonian

We are now in a position to write down the Hamiltonian for the complete system. In the Schrödinger picture, the Hamiltonian is:

$$\begin{aligned}\hat{H} = {} & \mathrm{i}\hbar\mathscr{E}\left(\hat{a}^\dagger e^{-\mathrm{i}\omega_L t} - \hat{a}e^{\mathrm{i}\omega_L t}\right) + \hbar\omega_a\hat{a}^\dagger\hat{a} + \hbar\omega_b\hat{b}^\dagger\hat{b} \\ & + \sum_{m_F=-4}^{4}\left(-\frac{\hbar\omega_A}{2} + g_{F,g}\mu_B m_F B\right)|g,m_F\rangle\langle g,m_F| \\ & + \sum_{m_F=-5}^{5}\left(+\frac{\hbar\omega_A}{2} + g_{F,e}\mu_B m_F B\right)|e,m_F\rangle\langle e,m_F| \\ & - \mathrm{i}\hbar g\left(\hat{a}\hat{\Sigma}_0^\dagger - \hat{a}^\dagger\hat{\Sigma}_0\right) - \mathrm{i}\hbar g\left(\hat{b}\left[\frac{\hat{\Sigma}_{-1}^\dagger + \hat{\Sigma}_{+1}^\dagger}{\sqrt{2}}\right] - \hat{b}^\dagger\left[\frac{\hat{\Sigma}_{-1} + \hat{\Sigma}_{+1}}{\sqrt{2}}\right]\right).\end{aligned} \tag{2.55}$$

In the experiment we are modelling, $\omega_A = \omega_a = \omega_b = \omega_0$ [5, 6]. In a frame rotating at the laser frequency, therefore, this becomes:

$$\begin{aligned}\hat{H} = {} & \mathrm{i}\hbar\mathscr{E}\left(\hat{a}^\dagger - \hat{a}\right) + \hbar(\omega_0-\omega_L)\hat{a}^\dagger\hat{a} + \hbar(\omega_0-\omega_L)\hat{b}^\dagger\hat{b} \\ & + \sum_{m_F=-4}^{4}\left(-\frac{\hbar(\omega_0-\omega_L)}{2} + g_{F,g}\mu_B m_F B\right)|g,m_F\rangle\langle g,m_F| \\ & + \sum_{m_F=-5}^{5}\left(+\frac{\hbar(\omega_0-\omega_L)}{2} + g_{F,e}\mu_B m_F B\right)|e,m_F\rangle\langle e,m_F| \\ & - \mathrm{i}\hbar g\left(\hat{a}\hat{\Sigma}_0^\dagger - \hat{a}^\dagger\hat{\Sigma}_0\right) - \mathrm{i}\hbar g\left(\hat{b}\left[\frac{\hat{\Sigma}_{-1}^\dagger + \hat{\Sigma}_{+1}^\dagger}{\sqrt{2}}\right] - \hat{b}^\dagger\left[\frac{\hat{\Sigma}_{-1} + \hat{\Sigma}_{+1}}{\sqrt{2}}\right]\right).\end{aligned} \tag{2.56}$$

Finally, in the experiment being modelled, the laser is tuned to the lower vacuum Rabi resonance, giving $\omega_L = \omega_0 - g$. In this case the Hamiltonian becomes:

$$\begin{aligned}\hat{H} = \mathrm{i}\hbar\mathscr{E}\left(\hat{a}^\dagger - \hat{a}\right) + \hbar g\hat{a}^\dagger\hat{a} + \hbar g\hat{b}^\dagger\hat{b} \\ + \sum_{m_F=-4}^{4}\left(-\frac{\hbar g}{2} + g_{F,g}\mu_B m_F B\right)|g,m_F\rangle\langle g,m_F| \\ + \sum_{m_F=-5}^{5}\left(+\frac{\hbar g}{2} + g_{F,e}\mu_B m_F B\right)|e,m_F\rangle\langle e,m_F| \\ - \mathrm{i}\hbar g\left(\hat{a}\hat{\Sigma}_0^\dagger - \hat{a}^\dagger\hat{\Sigma}_0\right) - \mathrm{i}\hbar g\left(\hat{b}\left[\frac{\hat{\Sigma}_{-1}^\dagger + \hat{\Sigma}_{+1}^\dagger}{\sqrt{2}}\right] - \hat{b}^\dagger\left[\frac{\hat{\Sigma}_{-1} + \hat{\Sigma}_{+1}}{\sqrt{2}}\right]\right). \quad (2.57)\end{aligned}$$

Chapter 3

Open quantum systems

If it were the case that the experiment we are modelling consisted of a simple closed quantum system, it would be sufficient to use the system Hamiltonian we have derived in conjunction with the Schrödinger equation to describe the dynamics of the system. However in this experiment, light can escape the cavity by spontaneous emission of the atom, or by leaking out through the cavity mirrors. In fact the light that leaks out of one of the cavity mirrors is what is measured in this experiment, making it an important part of the system. Consequently it is not sufficient to model a simple closed system.

An open quantum system is a quantum mechanical system which interacts with a second, external quantum system — the surrounding environment, known as the reservoir, and denoted R. An open quantum system S can be considered to be part of a larger closed system $S \otimes R$. The combined system has density operator $\chi(t)$, the time evolution of which is described by the Schrödinger equation for a density matrix (also known as the von Neumann equation):

$$\dot{\chi}(t) = \frac{1}{\mathrm{i}\hbar}\left[\hat{H}_{S\otimes R}, \chi(t)\right]. \tag{3.1}$$

However, we wish to investigate the system S without requiring detailed information about the composite system $S \otimes R$, particularly considering the complexity of the reservoir R. We can use the reduced density operator $\rho(t)$, defined by

$$\rho(t) \equiv \mathrm{tr}_R\left[\chi(t)\right], \tag{3.2}$$

where the trace is taken over the reservoir states. If $\hat{O}$ is an operator in the Hilbert space of S we can calculate its expectation value in the Schrödinger picture using only $\rho(t)$, as opposed to the full $\chi(t)$:

$$\langle\hat{O}\rangle = \mathrm{tr}_{S\otimes R}\left[\hat{O}\chi(t)\right] = \mathrm{tr}_S\left[\hat{O}\mathrm{tr}_R\left[\chi(t)\right]\right] = \mathrm{tr}_S\left[\hat{O}\rho(t)\right]. \tag{3.3}$$

Therefore, we require an equation for $\rho(t)$ into which the properties of R enter only as parameters. This equation of motion is known as the *master equation*.

3.1 Derivation of the master equation

The master equation that we will use to perform numerical simulations is required to be in *Lindblad form*, and is also known as the *Lindblad equation*. This equation has similar form to the Schrödinger equation, but with additional terms which describe the relaxation of S towards equilibrium with R:

$$\dot{\rho}(t) = \frac{1}{\mathrm{i}\hbar}\left[\hat{H}_S, \hat{\rho}(t)\right] + \text{decay terms}. \tag{3.4}$$

We will now present a brief derivation of the master equation in Lindblad form.

3.1.1 The integro-differential Schrödinger equation

We begin by decomposing the Hamiltonian for the composite system as follows

$$H_{S\otimes R} = H_S + H_R + H_{SR} \tag{3.5}$$

where H_S and H_R are the Hamiltonians for S and R, respectively, and H_{SR} is an interaction Hamiltonian.

We can transform the Schrödinger equation (Eq. (3.1)) into an interaction picture to separate the motion generated by $H_S + H_R$ from the motion generated by the interaction Hamiltonian H_{SR}. We introduce the transformed density operator,

$$\tilde{\chi}(t) = e^{(\mathrm{i}/\hbar)(H_S+H_R)t}\,\chi(t)e^{-(\mathrm{i}/\hbar)(H_S+H_R)t}, \tag{3.6}$$

which gives us a transformed Schrödinger equation,

$$\dot{\tilde{\chi}} = \frac{1}{\mathrm{i}\hbar}\left[\tilde{H}_{SR}(t), \tilde{\chi}\right], \tag{3.7}$$

with

$$\tilde{H}_{SR}(t) \equiv e^{(\mathrm{i}/\hbar)(H_S+H_R)t}\,H_{SR}(t)e^{-(\mathrm{i}/\hbar)(H_S+H_R)t}. \tag{3.8}$$

We integrate Eq. (3.7) formally to give

$$\tilde{\chi}(t) = \chi(0) + \frac{1}{\mathrm{i}\hbar}\int_0^t \mathrm{d}t'\left[\tilde{H}_{SR}(t'), \tilde{\chi}(t')\right], \tag{3.9}$$

and substitute back into Eq. (3.7) to obtain

$$\dot{\tilde{\chi}} = \frac{1}{\mathrm{i}\hbar}\left[\tilde{H}_{SR}(t), \chi(0)\right] - \frac{1}{\hbar^2}\int_0^t \mathrm{d}t'\left[\tilde{H}_{SR}(t), \left[\tilde{H}_{SR}(t'), \tilde{\chi}(t')\right]\right], \tag{3.10}$$

which is an exact equation for the time evolution of the density matrix in the interaction picture, written in integro-differential form. In this form it is convenient to make approximations to obtain a useful master equation.

3.1.2 The master equation for the reduced density operator

In Eq. (3.2), the reduced density operator was defined. By taking the trace of the right hand side of Eq. (3.10) over the reservoir states, we can obtain an expression for the reduced density operator in the interaction picture, known as the master equation:

$$\dot{\tilde{\rho}} = \frac{1}{\mathrm{i}\hbar}\mathrm{tr}_R\left\{\left[\tilde{H}_{SR}(t), \tilde{\chi}(0)\right]\right\} - \frac{1}{\hbar^2}\int_0^t \mathrm{d}t'\,\mathrm{tr}_R\left\{\left[\tilde{H}_{SR}(t), \left[\tilde{H}_{SR}(t'), \tilde{\chi}(t')\right]\right]\right\}. \tag{3.11}$$

We assume that the interaction is turned on at $t = 0$ and that the system and reservoir are initially uncorrelated. Then $\chi(0) = \tilde{\chi}(0)$ can be written

$$\chi(0) = \rho(0)R_0 \tag{3.12}$$

where R_0 is the initial density operator of the reservoir. Assuming the condition

$$\mathrm{tr}_R\left[\tilde{H}_{SR}(t)R_0\right] = 0, \tag{3.13}$$

which can always be arranged by including $\mathrm{tr}_R[H_{SR}(t)R_0]$ in the system Hamiltonian [7], we can eliminate the first term in Eq. (3.11), giving

$$\dot{\tilde{\rho}} = -\frac{1}{\hbar^2}\int_0^t \mathrm{d}t'\,\mathrm{tr}_R\left\{\left[\tilde{H}_{SR}(t), \left[\tilde{H}_{SR}(t'), \tilde{\chi}(t')\right]\right]\right\}. \tag{3.14}$$

3.1.3 The Born approximation

If there were no interaction between the system and the reservoir, $\tilde{\chi}(t)$ could be written as a direct product at all times. However correlations between S and R will arise at later times due to the interaction H_{SR}. We assume that the interaction is weak, so that at all times $\tilde{\chi}(t)$ will deviate from an uncorrelated state by terms of order H_{SR}:

$$\tilde{\chi}(t) = \tilde{\rho}(t)R_0 + \mathcal{O}(H_{SR}). \tag{3.15}$$

Now we make the *Born approximation* by neglecting terms higher than second order in H_{SR}. This enables us to write the master equation, Eq. (3.14), as

$$\dot{\tilde{\rho}} = -\frac{1}{\hbar^2}\int_0^t \mathrm{d}t'\,\mathrm{tr}_R\left\{\left[\tilde{H}_{SR}(t),\left[\tilde{H}_{SR}(t'),\tilde{\rho}(t')R_0\right]\right]\right\}. \tag{3.16}$$

3.1.4 The Markov approximation

Equation (3.16) is not Markovian: the future evolution of $\tilde{\rho}(t)$ depends on its past history through the integration over t'. The future evolution of a Markovian system depends only on its present state. It is desirable to make a *Markov approximation* so that the master equation is Markovian.

Potentially, the state of S can depend on its past history due to its interaction with the reservoir. The system can effect changes in the reservoir which are later "reflected" back on the future evolution of the system. However the reservoir is typically a large system with many degrees of freedom, maintained in thermal equilibrium. In this case we expect the reservoir to be essentially unaffected by its interaction with the system. Thus we can neglect all past values of $\tilde{\rho}(t)$ when evaluating its future evolution. The master equation now becomes

$$\dot{\tilde{\rho}} = -\frac{1}{\hbar^2}\int_0^t \mathrm{d}t'\,\mathrm{tr}_R\left\{\left[\tilde{H}_{SR}(t),\left[\tilde{H}_{SR}(t'),\tilde{\rho}(t)R_0\right]\right]\right\} \tag{3.17}$$

where we have replaced $\tilde{\rho}(t')R_0$ with $\tilde{\rho}(t)R_0$ so that we do not integrate over the past history of $\tilde{\rho}$.

3.1.5 Master equation in Lindblad form

We make the model more specific by writing

$$H_{SR} = \hbar\sum_i s_i\Gamma_i \tag{3.18}$$

where the s_i are operators in the Hilbert space of S, and the Γ_i are operators in the Hilbert space of R. Then

$$\begin{aligned}\tilde{H}_{SR}(t) &= \hbar\sum_i e^{(\mathrm{i}/\hbar)(H_S+H_R)t}\,s_i\Gamma_i\,e^{-(\mathrm{i}/\hbar)(H_S+H_R)t}\\ &= \hbar\sum_i\left(e^{(\mathrm{i}/\hbar)H_St}\,s_i\,e^{-(\mathrm{i}/\hbar)H_St}\right)\left(e^{(\mathrm{i}/\hbar)H_Rt}\,\Gamma_i\,e^{-(\mathrm{i}/\hbar)H_Rt}\right)\\ &= \hbar\sum_i\tilde{s}_i(t)\tilde{\Gamma}_i(t)\end{aligned} \tag{3.19}$$

We substitute this interaction Hamiltonian into the master equation in the Born-Markov approximation (3.17), to obtain

$$\dot{\tilde{\rho}} = -\sum_i\sum_j\int_0^t \mathrm{d}t'\,\mathrm{tr}_R\left\{\left[\tilde{s}_i(t)\tilde{\Gamma}_i(t),\left[\tilde{s}_j(t')\tilde{\Gamma}_j(t'),\tilde{\rho}(t)R_0\right]\right]\right\}. \tag{3.20}$$

Evaluating commutators, noting that the trace is taken only over the reservoir variables and operators, and using the cyclic property of the trace — $\mathrm{tr}(\hat{A}\hat{B}\hat{C}) = \mathrm{tr}(\hat{C}\hat{A}\hat{B}) = \mathrm{tr}(\hat{B}\hat{C}\hat{A})$ — allows us to write this as

$$\dot{\tilde{\rho}} = -\sum_i \sum_j \int_0^t \mathrm{d}t' \, \Big[\Big(\tilde{s}_i(t)\tilde{s}_j(t')\tilde{\rho}(t) - \tilde{s}_j(t')\tilde{\rho}(t)\tilde{s}_i(t) \Big) \mathrm{tr}_R \left\{ R_0 \tilde{\Gamma}_i(t) \tilde{\Gamma}_j(t') \right\} + \Big(\tilde{\rho}(t)\tilde{s}_j(t')\tilde{s}_i(t) - \tilde{s}_i(t)\tilde{\rho}(t)\tilde{s}_j(t') \Big) \mathrm{tr}_R \left\{ R_0 \tilde{\Gamma}_j(t') \tilde{\Gamma}_i(t) \right\} \Big] . \quad (3.21)$$

At this point we replace some of the Hermitian $\tilde{H}_{SR}$ terms with their adjoints (this is possible because each term must be present along with its adjoint in H_{SR}, to make the interaction Hamiltonian Hermitian); this will allow notational simplifications later on [15]:

$$\dot{\tilde{\rho}} = -\sum_i \sum_j \int_0^t \mathrm{d}t' \, \Big[\Big(\tilde{s}_i^\dagger(t)\tilde{s}_j(t')\tilde{\rho}(t) - \tilde{s}_j(t')\tilde{\rho}(t)\tilde{s}_i^\dagger(t) \Big) \mathrm{tr}_R \left\{ R_0 \tilde{\Gamma}_i^\dagger(t) \tilde{\Gamma}_j(t') \right\} + \Big(\tilde{\rho}(t)\tilde{s}_j^\dagger(t')\tilde{s}_i(t) - \tilde{s}_i(t)\tilde{\rho}(t)\tilde{s}_j^\dagger(t') \Big) \mathrm{tr}_R \left\{ R_0 \tilde{\Gamma}_j^\dagger(t') \tilde{\Gamma}_i(t) \right\} \Big] . \quad (3.22)$$

In the interaction picture the time-evolution of the $\tilde{s}_i$ is governed by a Heisenberg-like equation of motion:

$$\dot{\tilde{s}}_i = \frac{1}{\mathrm{i}\hbar} [\tilde{s}_i, H_S] . \quad (3.23)$$

It is assumed that the initial Hamiltonian is constructed in terms of s_i in such a way that Eq. (3.23) has solutions of the form

$$\tilde{s}_i = s_i e^{-\mathrm{i}\omega_i t} . \quad (3.24)$$

Thus, we can substitute the time dependence of $\tilde{s}_i$ into Eq. (3.22), and apply the so-called *secular approximation*, neglecting the rapidly oscillating terms for which $i \neq j$. Furthermore we write the traces as expectation values, to obtain

$$\dot{\tilde{\rho}} = -\sum_j \left[\left(s_j^\dagger s_j \tilde{\rho}(t) - s_j \tilde{\rho}(t) s_j^\dagger \right) \int_0^t \mathrm{d}t' \, \langle \tilde{\Gamma}_j^\dagger(t) \tilde{\Gamma}_j(t') \rangle_R + \left(\tilde{\rho}(t) s_j^\dagger s_j - s_j \tilde{\rho}(t) s_j^\dagger \right) \int_0^t \mathrm{d}t' \, \langle \tilde{\Gamma}_j^\dagger(t') \tilde{\Gamma}_j(t) \rangle_R \right] . \quad (3.25)$$

Now we define

$$\gamma_j = \int_0^t \mathrm{d}t' \, \langle \tilde{\Gamma}_j^\dagger(t) \tilde{\Gamma}_j(t') \rangle_R + \mathrm{h.c.} \quad (3.26)$$

where h.c. denotes the Hermitian conjugate. If we take $\langle \tilde{\Gamma}_j^\dagger(t) \tilde{\Gamma}_j(t') \rangle_R$ to be real, we have

$$\dot{\tilde{\rho}} = -\sum_j \frac{\gamma_j}{2} \left(-2 s_j \tilde{\rho}(t) s_j^\dagger + s_j^\dagger s_j \tilde{\rho}(t) + \tilde{\rho}(t) s_j^\dagger s_j \right) . \quad (3.27)$$

We now use

$$\dot{\rho} = \frac{1}{\mathrm{i}\hbar} [H_S, \rho(t)] + e^{-(\mathrm{i}/\hbar)H_S t} \, \dot{\tilde{\rho}} \, e^{(\mathrm{i}/\hbar)H_S t} \quad (3.28)$$

to transform Eq. (3.27) back into the Schrödinger picture, which finally yields the master equation in Lindblad form (also known as the Lindblad equation):

$$\dot{\rho} = \frac{1}{\mathrm{i}\hbar} [H_S, \rho(t)] + \sum_j \frac{\gamma_j}{2} \left(2 s_j \rho(t) s_j^\dagger - s_j^\dagger s_j \rho(t) - \rho(t) s_j^\dagger s_j \right) . \quad (3.29)$$

The master equation in Lindblad form is conveniently expressed in terms of *collapse operators* (or *jump operators*), $\hat{C}_k = \sqrt{\gamma_k}\hat{s}_k$:

$$\frac{\partial \hat{\rho}}{\partial t} = \frac{1}{\mathrm{i}\hbar}\left[\hat{H}_S, \hat{\rho}\right] + \sum_k \left(\hat{C}_k \hat{\rho} \hat{C}_k^\dagger - \frac{1}{2}\hat{C}_k^\dagger \hat{C}_k \hat{\rho} - \frac{1}{2}\hat{\rho}\hat{C}_k^\dagger \hat{C}_k \right). \tag{3.30}$$

Another way to express the master equation is using the Liouvillian superoperator $\mathscr{L}$:

$$\dot{\rho}(t) = \mathscr{L}\rho(t) \tag{3.31}$$

where the superoperator $\mathscr{L}$ is a linear operator that acts on other operators rather than on state vectors. For our master equation, $\mathscr{L}$ is given by

$$\mathscr{L}\cdot = \frac{1}{\mathrm{i}\hbar}\left[\hat{H}_S, \cdot\right] + \sum_k \left(\hat{C}_k \cdot \hat{C}_k^\dagger - \frac{1}{2}\hat{C}_k^\dagger \hat{C}_k \cdot - \frac{1}{2}\cdot \hat{C}_k^\dagger \hat{C}_k \right). \tag{3.32}$$

The superoperator form of the master equation will be useful when we come to perform simulations.

3.2 Master equation for the cavity QED system

To formulate the master equation for the system we will be simulating, we use the master equation in Lindblad form given by Eq. (3.30) with the system Hamiltonian H_S given by Eq. (2.57). It remains to find the appropriate collapse operators $\hat{C}_k$ for our model.

The strength of the atom-cavity interaction is determined by three parameters:

- the cavity mode decay rate κ,
- the atomic decay rate γ,
- the atom-cavity coupling constant g.

The cavity mode decay rate κ leads to collapse operators which relate to light leaking out of the cavity through the cavity mirrors, given by:

$$\hat{C}_a = \sqrt{2\kappa}\hat{a}, \tag{3.33a}$$

$$\hat{C}_b = \sqrt{2\kappa}\hat{b}. \tag{3.33b}$$

The factor of two comes from the fact that κ is defined to correspond to the parameter $\gamma_j/2$ in Eq. (3.29).

The atomic decay rate γ leads to collapse operators which relate to spontaneous emission of light from the atom. The decay rate is in reality determined by several factors, but we will take it to represent only the emission of a photon of the resonant frequency in a direction other than that of the cavity mode. Other processes, for example the atom decaying to other levels, represent a breakdown of the two-level atom approximation we are using, and will thus not be considered. Atomic transitions with different Δm_F refer to light with different polarisation, coupled to independent reservoirs. Thus we will have three collapse operators for the three $\Delta m_F = 0, \pm 1$ transitions:

$$\hat{C}_{-1} = \sqrt{\gamma}\hat{\Sigma}_{-1}, \tag{3.34a}$$

$$\hat{C}_0 = \sqrt{\gamma}\hat{\Sigma}_0, \tag{3.34b}$$

$$\hat{C}_{+1} = \sqrt{\gamma}\hat{\Sigma}_{+1}. \tag{3.34c}$$

Carrying the sum in Eq. (3.30) over all five of the collapse operators given in Eqs. (3.33) and (3.34) gives the complete master equation in Lindblad form for this system.

3.3 Quantum regression formula

The master equation gives us an explicit formula for the time dependence of the reduced density operator $\rho(t)$, defined in Eq. (3.2). Thus we can calculate the time dependence of any operator $\hat{O}$ in the Hilbert space of S using Eq. (3.3). However evaluating two-time averages of the form

$$\langle \hat{O}_1(t)\hat{O}_2(t')\hat{O}_3(t)\rangle \quad \text{with} \quad t'-t \geq 0 \tag{3.35}$$

is more difficult. In the Schrödinger picture, operators are generally time-independent, so such an expression cannot be evaluated. In the Heisenberg picture, however, operators have an explicit time dependence, so to evaluate such a two-time average we can write the average as a trace in the Heisenberg picture, and then transform the trace back into the Schrödinger picture. The average in the Heisenberg picture is given by

$$\begin{aligned}\langle \hat{O}_1(t)\hat{O}_2(t')\hat{O}_3(t)\rangle &= \mathrm{tr}_{S\otimes R}\left[\chi^{(H)}\hat{O}_1^{(H)}(t)\hat{O}_2^{(H)}(t')\hat{O}_3^{(H)}(t)\right] \\ &= \mathrm{tr}_{S\otimes R}\left[\chi^{(H)}e^{(\mathrm{i}/\hbar)Ht}\hat{O}_1^{(S)}e^{(\mathrm{i}/\hbar)H(t'-t)}\hat{O}_2^{(S)}e^{-(\mathrm{i}/\hbar)H(t'-t)}\hat{O}_3^{(S)}e^{-(\mathrm{i}/\hbar)Ht}\right].\end{aligned} \tag{3.36}$$

Using the cyclic property of the trace, this becomes

$$\begin{aligned}\langle \hat{O}_1(t)\hat{O}_2(t')\hat{O}_3(t)\rangle &= \mathrm{tr}_{S\otimes R}\left[\hat{O}_2^{(S)}e^{-(\mathrm{i}/\hbar)H(t'-t)}\hat{O}_3^{(S)}e^{-(\mathrm{i}/\hbar)Ht}\chi^{(H)}e^{(\mathrm{i}/\hbar)Ht}\hat{O}_1^{(S)}e^{(\mathrm{i}/\hbar)H(t'-t)}\right] \\ &= \mathrm{tr}_{S\otimes R}\left[\hat{O}_2^{(S)}e^{-(\mathrm{i}/\hbar)H(t'-t)}\hat{O}_3^{(S)}\chi^{(S)}(t)\hat{O}_1^{(S)}e^{(\mathrm{i}/\hbar)H(t'-t)}\right] \\ &= \mathrm{tr}_S\left[\hat{O}_2\,\mathrm{tr}_R\left[e^{-(\mathrm{i}/\hbar)H(t'-t)}\hat{O}_3\chi(t)\hat{O}_1e^{(\mathrm{i}/\hbar)H(t'-t)}\right]\right]\end{aligned} \tag{3.37}$$

where we have used the fact that $\hat{O}_2$ is an operator in the Hilbert space of S alone. We now define

$$\chi_{\hat{O}_3\hat{O}_1}(\tau) \equiv e^{-(\mathrm{i}/\hbar)H\tau}\hat{O}_3\chi(t)\hat{O}_1e^{(\mathrm{i}/\hbar)H\tau} \quad \text{with} \quad \tau \equiv t'-t \tag{3.38}$$

so as to obtain

$$\langle \hat{O}_1(t)\hat{O}_2(t')\hat{O}_3(t)\rangle = \mathrm{tr}_S\left[\hat{O}_2\,\mathrm{tr}_R\left[\chi_{\hat{O}_3\hat{O}_1}(\tau)\right]\right]. \tag{3.39}$$

We now define the reduced density operator

$$\rho_{\hat{O}_3\hat{O}_1}(\tau) \equiv \mathrm{tr}_R\left[\chi_{\hat{O}_3\hat{O}_1}(\tau)\right] \tag{3.40}$$

and, using the assumption contained in Eq. (3.15), i.e. $\chi(t) = R_0\rho(t)$, we find

$$\begin{aligned}\chi_{\hat{O}_3\hat{O}_1}(0) &= \hat{O}_3\chi(t)\hat{O}_1 \\ &= R_0\hat{O}_3\rho(t)\hat{O}_1 \\ &= R_0\mathrm{tr}_R\left[\hat{O}_3\chi(t)\hat{O}_1\right] \\ &= R_0\mathrm{tr}_R\left[\rho_{\hat{O}_3\hat{O}_1}(0)\right] \\ &= R_0\rho_{\hat{O}_3\hat{O}_1}(0).\end{aligned} \tag{3.41}$$

Finally, $\chi_{\hat{O}_3\hat{O}_1}$ clearly satisfies the equation

$$\frac{\mathrm{d}}{\mathrm{d}\tau}\chi_{\hat{O}_3\hat{O}_1}(\tau) = \frac{1}{\mathrm{i}\hbar}\left[\hat{H},\chi_{\hat{O}_3\hat{O}_1}(\tau)\right]. \tag{3.42}$$

Equations (3.40), (3.41) and (3.42) are now equivalent to (3.2), (3.12) and (3.7) respectively, which were our starting points for the derivation of the master equation. Since the Schrödinger equations

for $\chi(t)$ and $\chi_{\hat{O}_3\hat{O}_1}(\tau)$ share the same Hamiltonian, we can follow an analogous path to the derivation of the master equation in the Born and Markov approximations. The resulting equation is

$$\frac{\mathrm{d}}{\mathrm{d}\tau}\rho_{\hat{O}_3\hat{O}_1}(\tau) = \mathscr{L}\rho_{\hat{O}_3\hat{O}_1}(\tau) \tag{3.43}$$

with formal solution

$$\rho_{\hat{O}_3\hat{O}_1}(\tau) = e^{\mathscr{L}\tau}\left(\rho_{\hat{O}_3\hat{O}_1}(0)\right) = e^{\mathscr{L}\tau}\left(\hat{O}_3\rho(0)\hat{O}_1\right). \tag{3.44}$$

Thus, Eq. (3.39) simplifies to give us the *quantum regression formula*

$$\langle\hat{O}_1(t)\hat{O}_2(t+\tau)\hat{O}_3(t)\rangle = \mathrm{tr}_S\left[\hat{O}_2\, e^{\mathscr{L}\tau}\left(\hat{O}_3\rho(t)\hat{O}_1\right)\right] \tag{3.45}$$

where the reduced density operator $\rho(t)$ satisfies the master equation $\dot{\rho}(t) = \mathscr{L}\rho(t)$.

Chapter 4

Cavity quantum electrodynamics

4.1 The Jaynes-Cummings model

In §2.1, we considered the Jaynes-Cummings model for a two-level atom coupled to a single cavity mode, with dipole coupling constant g, and derived the Hamiltonian for this system given in Eq. (2.26). For the case where the incident light, of frequency ω, is resonant with the atomic transition, we have for the Jaynes-Cummings Hamiltonian:

$$\hat{H} = \frac{\hbar\omega}{2}\hat{\sigma}_z + \hbar\omega\hat{a}^\dagger\hat{a} - \mathrm{i}\hbar g\left(\hat{a}\hat{\sigma}_+ - \hat{a}^\dagger\hat{\sigma}_-\right). \tag{4.1}$$

The system ground state is $|g\rangle|0\rangle$, and has energy $-\frac{1}{2}\hbar\omega$. We consider first the 'bare' states of an uncoupled resonant system. In this case, all excited states are doubly degenerate. The first excited state is at energy $\frac{1}{2}\hbar\omega$; the corresponding eigenstates of the Hamiltonian Eq. (4.1) are those with either the atom in the excited state and no photons in the cavity, $|e\rangle|0\rangle$, or with the atom in the ground state and one photon in the cavity, $|g\rangle|1\rangle$. The n^{th} excited state (where $n > 0$) has energy $\left(n - \frac{1}{2}\right)\hbar\omega$; its corresponding eigenstates are $|g\rangle|n\rangle$ and $|e\rangle|n-1\rangle$.

The electric-dipole interaction between the atom and the cavity, whose Hamiltonian is given by

$$\hat{H}_I = -\mathrm{i}\hbar g\left(\hat{a}\hat{\sigma}_+ - \hat{a}^\dagger\hat{\sigma}_-\right), \tag{4.2}$$

couples the degenerate states and lifts the degeneracy. In particular, we have

$$\hat{H}|g\rangle|n\rangle = \left(n - \frac{1}{2}\right)\hbar\omega|g\rangle|n\rangle - \mathrm{i}\hbar g\sqrt{n}|e\rangle|n-1\rangle, \tag{4.3a}$$

$$\hat{H}|e\rangle|n-1\rangle = \left(n - \frac{1}{2}\right)\hbar\omega|e\rangle|n-1\rangle + \mathrm{i}\hbar g\sqrt{n}|g\rangle|n\rangle, \tag{4.3b}$$

for all $n > 0$ (i.e. above the ground state). When the interaction is applied, the excited states are mixed; they are linear combinations of the eigenstates of the uncoupled system:

$$|E_n\rangle = a_n|g\rangle|n\rangle + b_n|e\rangle|n-1\rangle. \tag{4.4}$$

The eigenstates of the coupled system satisfy

$$\hat{H}|E_n\rangle = E_n|E_n\rangle. \tag{4.5}$$

Using Eqs. (4.3), we can write an equation relating the coefficients a_n and b_n and the energy eigenvalues E_n:

$$a_n\left[\left(n - \frac{1}{2}\right)\hbar\omega|g\rangle|n\rangle - \mathrm{i}\hbar g\sqrt{n}|e\rangle|n-1\rangle\right] + b_n\left[\left(n - \frac{1}{2}\right)\hbar\omega|e\rangle|n-1\rangle + \mathrm{i}\hbar g\sqrt{n}|g\rangle|n\rangle\right] = E_n\left[a_n|g\rangle|n\rangle + b_n|e\rangle|n-1\rangle\right], \tag{4.6}$$

which gives the simultaneous equations

$$\begin{pmatrix} \left(n-\frac{1}{2}\right)\hbar\omega & \mathrm{i}\hbar g\sqrt{n} \\ -\mathrm{i}\hbar g\sqrt{n} & \left(n-\frac{1}{2}\right)\hbar\omega \end{pmatrix} \begin{pmatrix} a_n \\ b_n \end{pmatrix} = E_n \begin{pmatrix} a_n \\ b_n \end{pmatrix}. \tag{4.7}$$

If we now define

$$\lambda_n = E_n - \left(n-\frac{1}{2}\right)\hbar\omega, \tag{4.8}$$

the equations to solve are

$$\begin{pmatrix} -\lambda_n & \mathrm{i}\hbar g\sqrt{n} \\ -\mathrm{i}\hbar g\sqrt{n} & -\lambda_n \end{pmatrix} \begin{pmatrix} a_n \\ b_n \end{pmatrix} = \mathbf{0}. \tag{4.9}$$

The characteristic equation is

$$\begin{vmatrix} -\lambda_n & \mathrm{i}\hbar g\sqrt{n} \\ -\mathrm{i}\hbar g\sqrt{n} & -\lambda_n \end{vmatrix} = \lambda_n^2 - n\hbar^2 g^2 = 0 \tag{4.10}$$

with solution

$$\lambda_n = \pm\sqrt{n}\hbar g. \tag{4.11}$$

Therefore the excited state energies are given by

$$E_n^{\pm} = \left(n-\frac{1}{2}\right)\hbar\omega \pm \sqrt{n}\hbar g. \tag{4.12}$$

Substituting back into Eq. (4.9) and solving for a_n and b_n gives the mixed atom-photon states

$$|E_n^+\rangle = \frac{1}{\sqrt{2}}\left(|g\rangle|n\rangle - \mathrm{i}|e\rangle|n-1\rangle\right), \tag{4.13a}$$

$$|E_n^-\rangle = \frac{1}{\sqrt{2}}\left(|g\rangle|n\rangle + \mathrm{i}|e\rangle|n-1\rangle\right). \tag{4.13b}$$

These mixed atom-photon states are known as the dressed states, and the ladder of doublets is known as the Jaynes-Cummings ladder. The Jaynes-Cummings ladder, and the relationships between the atomic states, photon number states, and dressed states, are illustrated in Fig. 4.1.

4.2 Photon correlation functions: analytic investigations

Consider a two-level atom coupled to a single cavity mode with dipole coupling constant g, as in the Jaynes-Cummings model. A system of this sort driven by a coherent laser field has Hamiltonian

$$\hat{H}_S = \mathrm{i}\hbar\mathscr{E}\left(\hat{a}^\dagger - \hat{a}\right) + \hbar\Delta\omega|e\rangle\langle e| + \hbar\Delta\omega\hat{a}^\dagger\hat{a} - \mathrm{i}\hbar g\left(\hat{a}\hat{\sigma}_+ - \hat{a}^\dagger\hat{\sigma}_-\right), \tag{4.14}$$

in a frame rotating at the laser frequency; $\Delta\omega$ is the detuning of the laser from resonance with the atomic transition and the cavity mode (which have the same frequency). The zero of energy has been set at the energy of the system ground state for reasons which will become clear shortly.

In the weak excitation regime, certain approximations can be made which allow an analytic solution for the steady-state second-order photon correlation function to be obtained. A solution of this sort for the case of zero detuning is obtained in [8, §16.1]; we aim to generalise the calculation to the case of non-zero detuning.

Firstly, the term $-\mathrm{i}\hbar\mathscr{E}\hat{a}$ in Eq. (4.14) can be neglected, as it gives a contribution only at higher order in $\mathscr{E}$.

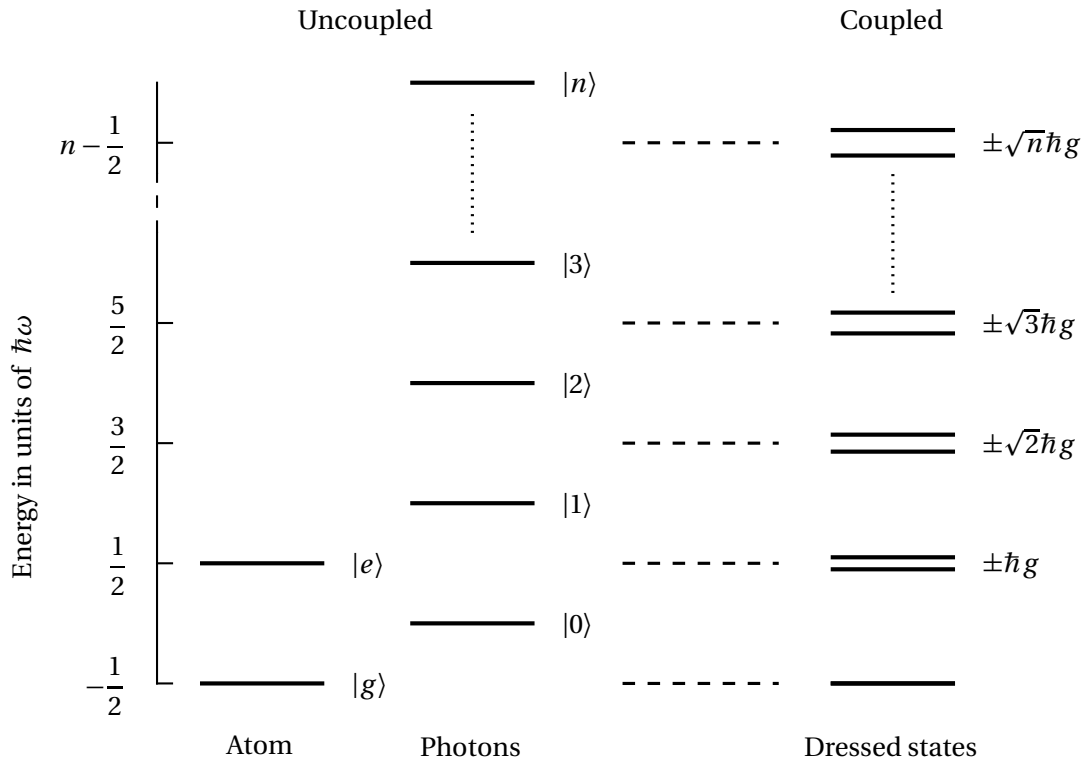

Figure 4.1: The Jaynes-Cummings ladder. Shown on the left are the energies of the uncoupled states of the atom and the field modes. Shown on the right is the ladder of dressed states, which describes a coupled atom-photon system with atom-cavity coupling constant g. Each "rung" of the ladder, except for the very lowest, comprises two dressed states.

We now want to simplify the master equation (Eq. (3.31)), with the Liouvillian given by Eq.(3.32). The collapse operators for this system are given by

$$\hat{C}_a = \sqrt{2\kappa}\hat{a} \tag{4.15a}$$

for the cavity mode, and

$$\hat{C}_a = \sqrt{\gamma}\hat{\sigma}_- \tag{4.15b}$$

for the two-level atom. The Liouvillian for this system is thus given by

$$\mathscr{L}\cdot = \frac{1}{\mathrm{i}\hbar}\left[\hat{H}_S,\cdot\right] + 2\kappa\left(\hat{a}\cdot\hat{a}^\dagger - \frac{1}{2}\hat{a}^\dagger\hat{a}\cdot - \frac{1}{2}\cdot\hat{a}^\dagger\hat{a}\right) + \gamma\left(\hat{\sigma}_-\cdot\hat{\sigma}_+ - \frac{1}{2}\hat{\sigma}_+\hat{\sigma}_-\cdot - \frac{1}{2}\cdot\hat{\sigma}_+\hat{\sigma}_-\right). \tag{4.16}$$

The terms in the Liouvillian (3.32) in $\hat{C}_k\cdot\hat{C}_k^\dagger$ represent collapses of the system related to its interaction with the environment. In this case specifically, $\hat{a}\cdot\hat{a}^\dagger$ and $\hat{\sigma}_-\cdot\hat{\sigma}_+$ represent light leaking out of the cavity through the cavity mirrors and spontaneous emission of the atom, respectively. In the case of very weak excitation of the system, the probability of interaction with the environment through photon emission is small, and the coherent time-evolution of the system is rarely interrupted by a collapse. As such, the system undergoes, to a good approximation, the time-evolution of a pure state. Mathematically, this approximation is equivalent to neglecting the terms in $\hat{C}_k\cdot\hat{C}_k^\dagger$ in the Liouvillian,

resulting in a modified Liouvillian $\mathscr{L}'$:

$$\mathscr{L}'\cdot = \frac{1}{\mathrm{i}\hbar}\left[\hat{H}_S,\cdot\right] - \frac{1}{2}\sum_k \left\{\hat{C}_k^\dagger \hat{C}_k,\cdot\right\} \tag{4.17}$$

where $\{\cdot,\cdot\}$ denotes the anti-commutator.

From the modified Liouvillian (4.17), we can formulate an approximate master equation:

$$\mathrm{i}\hbar\frac{\partial\rho}{\partial t} \approx \left[\hat{H}_S,\rho\right] - \mathrm{i}\hbar\frac{1}{2}\sum_k \left\{\hat{C}_k^\dagger \hat{C}_k,\rho\right\}. \tag{4.18}$$

We now define an effective Hamiltonian

$$\hat{H}_{\text{eff}} = \hat{H}_S - \mathrm{i}\hbar\frac{1}{2}\sum_k \hat{C}_k^\dagger \hat{C}_k, \tag{4.19}$$

and the state ket of the system $|\Psi(t)\rangle$ such that

$$\rho(t) = |\Psi(t)\rangle\langle\Psi(t)|, \tag{4.20}$$

and show that the effective Hamiltonian is consistent with the approximate master equation (Eq. (4.18)).

The effective Hamiltonian is non-Hermitian, and generates non-unitary time-evolution which does not preserve the norm of the state. However this approximation is acceptable as we only desire solutions correct to leading order in $\mathscr{E}$.

We have the dual correspondence given by

$$\hat{H}_{\text{eff}}|\Psi(t)\rangle \overset{\text{DC}}{\longleftrightarrow} \langle\Psi(t)|\hat{H}_{\text{eff}}^\dagger, \tag{4.21}$$

which, along with the Schrödinger equation,

$$\mathrm{i}\hbar\frac{\partial}{\partial t}|\Psi(t)\rangle = \hat{H}_{\text{eff}}|\Psi(t)\rangle, \tag{4.22}$$

gives the equation for the time-evolution of the state bra:

$$\mathrm{i}\hbar\frac{\partial}{\partial t}\langle\Psi(t)| = -\langle\Psi(t)|\hat{H}_{\text{eff}}^\dagger. \tag{4.23}$$

We can now differentiate the density operator and substitute in these results to obtain the master equation:

$$\begin{aligned}
\mathrm{i}\hbar\frac{\partial}{\partial t}\rho(t) &= \left[\mathrm{i}\hbar\frac{\partial}{\partial t}|\Psi(t)\rangle\right]\langle\Psi(t)| + |\Psi(t)\rangle\left[\mathrm{i}\hbar\frac{\partial}{\partial t}\langle\Psi(t)|\right] \\
&= \hat{H}_{\text{eff}}|\Psi(t)\rangle\langle\Psi(t)| - |\Psi(t)\rangle\langle\Psi(t)|\hat{H}_{\text{eff}}^\dagger \\
&= \left(\hat{H}_S - \mathrm{i}\hbar\frac{1}{2}\sum_k \hat{C}_k^\dagger\hat{C}_k\right)|\Psi(t)\rangle\langle\Psi(t)| - |\Psi(t)\rangle\langle\Psi(t)|\left(\hat{H}_S + \mathrm{i}\hbar\frac{1}{2}\sum_k \hat{C}_k^\dagger\hat{C}_k\right) \\
&= \hat{H}_S\rho(t) - \rho(t)\hat{H}_S - \mathrm{i}\hbar\frac{1}{2}\sum_k\left(\hat{C}_k^\dagger\hat{C}_k\rho(t) + \rho(t)\hat{C}_k^\dagger\hat{C}_k\right) \\
&= \left[\hat{H}_S,\rho(t)\right] - \mathrm{i}\hbar\frac{1}{2}\sum_k\left\{\hat{C}_k^\dagger\hat{C}_k,\rho(t)\right\},
\end{aligned} \tag{4.24}$$

which is, of course, the same as Eq. (4.18).

In the case of a driven two-level atom coupled to a cavity, the modified Liouvillian is given by

$$\mathscr{L}'\cdot = \frac{1}{\mathrm{i}\hbar}\left[\hat{H}_S,\cdot\right] - \kappa\left\{\hat{a}^\dagger\hat{a},\cdot\right\} - \frac{\gamma}{2}\left\{\hat{\sigma}_+\hat{\sigma}_-,\cdot\right\}, \tag{4.25}$$

which gives an effective Hamiltonian

$$\hat{H}_{\text{eff}} = \hat{H}_S - \mathrm{i}\hbar\left(\kappa\hat{a}^\dagger\hat{a} + \frac{\gamma}{2}\hat{\sigma}_+\hat{\sigma}_-\right), \tag{4.26}$$

and yields a non-unitary Schrödinger equation describing the coherent time-evolution between collapses due to photon emissions,

$$\frac{\partial}{\partial t}|\Psi\rangle = \left[\frac{\hat{H}_S}{\mathrm{i}\hbar} - \kappa\hat{a}^\dagger\hat{a} - \frac{\gamma}{2}\hat{\sigma}_+\hat{\sigma}_-\right]|\Psi\rangle, \tag{4.27}$$

with

$$\frac{\hat{H}_S}{\mathrm{i}\hbar} = \mathscr{E}\hat{a}^\dagger - \mathrm{i}\Delta\omega\hat{a}^\dagger\hat{a} - \mathrm{i}\Delta\omega|e\rangle\langle e| - g\left(\hat{a}\hat{\sigma}_+ - \hat{a}^\dagger\hat{\sigma}_-\right). \tag{4.28}$$

Written out in full, the non-unitary Schrödinger equation is

$$\frac{\partial}{\partial t}|\Psi\rangle = \left[\mathscr{E}\hat{a}^\dagger - \mathrm{i}\Delta\omega\hat{a}^\dagger\hat{a} - \mathrm{i}\Delta\omega|e\rangle\langle e| - g\left(\hat{a}|e\rangle\langle g| - \hat{a}^\dagger|g\rangle\langle e|\right) - \kappa\hat{a}^\dagger\hat{a} - \frac{\gamma}{2}|e\rangle\langle e|\right]|\Psi\rangle. \tag{4.29}$$

Now we must choose a basis in which to expand the system state. We neglect excitations of the cavity mode above the two-quantum level, as is also discussed in §5.3. Thus the basis we will use is

$$\left.\begin{aligned} &|g\rangle|0\rangle\\ &|g\rangle|1\rangle\\ &|g\rangle|2\rangle\\ &|e\rangle|0\rangle\\ &|e\rangle|1\rangle \end{aligned}\right\}, \tag{4.30}$$

which we will refer to as the *two-quantum basis for a single non-degenerate two-level atom in a single-mode cavity*. We expand the system state thus:

$$|\Psi\rangle = |g\rangle|0\rangle + \alpha(t)|g\rangle|1\rangle + \beta(t)|e\rangle|0\rangle + \eta(t)|g\rangle|2\rangle + \zeta(t)|e\rangle|1\rangle, \tag{4.31}$$

where the normalisation has been chosen so that the state amplitude of the ground state is unity at all times. This is an approximation, but it holds to leading order in $\mathscr{E}$ in the weak excitation regime, provided that the zero of energy is taken to be the energy of the ground state. This is done to ensure that there are no non-negligible terms in the equation of motion of the ground state, even for large detunings.

Substituting Eq. (4.31) into the non-unitary Schrödinger equation (Eq. (4.29)) yields the equations of motion for the state amplitudes:

$$\dot{\alpha} = -\kappa\alpha + g\beta - \mathrm{i}\Delta\omega\alpha + \mathscr{E}, \tag{4.32a}$$

$$\dot{\beta} = -\frac{\gamma}{2}\beta - g\alpha - \mathrm{i}\Delta\omega\beta, \tag{4.32b}$$

$$\dot{\eta} = -2\kappa\eta + \sqrt{2}g\zeta - 2\mathrm{i}\Delta\omega\eta + \sqrt{2}\mathscr{E}\alpha, \tag{4.32c}$$

$$\dot{\zeta} = -\kappa\zeta - \frac{\gamma}{2}\zeta - \sqrt{2}g\eta - 2\mathrm{i}\Delta\omega\zeta + \mathscr{E}\beta. \tag{4.32d}$$

We wish to compute the steady state driven mode self-correlation, given by

$$g^{(2)}_{aa}(\tau) = \frac{\langle \hat{a}^\dagger(0)\hat{a}^\dagger(\tau)\hat{a}(\tau)\hat{a}(0)\rangle_{\rm ss}}{\langle \hat{a}^\dagger\hat{a}\rangle_{\rm ss}\langle \hat{a}^\dagger\hat{a}\rangle_{\rm ss}}. \tag{4.33}$$

The quantum regression formula (3.45) implies that this can be calculated using

$$g^{(2)}_{aa}(\tau) = \frac{\langle \hat{a}^\dagger(\tau)\hat{a}(\tau)\rangle_{\rho(0)=\rho'_{\rm ss}}}{\langle \hat{a}^\dagger\hat{a}\rangle_{\rm ss}}, \tag{4.34}$$

with

$$\rho'_{\rm ss} = \frac{\hat{a}\rho_{\rm ss}\hat{a}^\dagger}{{\rm tr}\left[\hat{a}\rho_{\rm ss}\hat{a}^\dagger\right]} \tag{4.35}$$

where $\rho_{\rm ss}$ is the density matrix in the steady state.

We are taking the system to be in the steady state at time $\tau = 0$, at which time a photon is emitted through the cavity mirror, causing the state of the system to collapse to a reduced state which we will denote $|\psi\rangle$. With the initial state expanded in the two-quantum basis, the reduced state can be expanded in the one-quantum basis:

$$|\psi(\tau)\rangle = |g\rangle|0\rangle + \alpha(\tau)|g\rangle|1\rangle + \beta(\tau)|e\rangle|0\rangle. \tag{4.36}$$

Where $\alpha(\tau)$ and $\beta(\tau)$ obey the equations of motion (4.32a) and (4.32b). The second-order correlation function is written in terms of the system state using the above expansion of the reduced system state:

$$g^{(2)}_{aa}(\tau) = \frac{\langle\psi(\tau)|\hat{a}^\dagger\hat{a}|\psi(\tau)\rangle}{\langle\psi_{\rm ss}|\hat{a}^\dagger\hat{a}|\psi_{\rm ss}\rangle}. \tag{4.37}$$

The initial condition for the reduced state is given in terms of the initial system state, defined in Eq. (4.31), by

$$|\psi(0)\rangle = \frac{\hat{a}|\Psi_{\rm ss}\rangle}{\sqrt{\langle\Psi_{\rm ss}|\hat{a}^\dagger\hat{a}|\Psi_{\rm ss}\rangle}}, \tag{4.38}$$

which is consistent with Eq. (4.35).

Thus we have initial conditions for the state amplitudes appearing in Eq. (4.36):

$$\alpha(0) = \frac{\sqrt{2}\eta_{\rm ss}}{\alpha_{\rm ss}}, \tag{4.39a}$$

$$\beta(0) = \frac{\zeta_{\rm ss}}{\alpha_{\rm ss}}, \tag{4.39b}$$

where $\alpha_{\rm ss}$, $\beta_{\rm ss}$, $\eta_{\rm ss}$, and $\zeta_{\rm ss}$ solve the steady state equation (4.44). In the same way we obtain from Eqs. (4.36) and (4.37),

$$g^{(2)}_{aa}(\tau) = \frac{|\alpha(\tau)|^2}{|\alpha_{\rm ss}|^2}. \tag{4.40}$$

Now all that remains to do is to find the steady-state solution to Eqs. (4.32), then solve for $\alpha(\tau)$ using the initial conditions (4.39).

Equations (4.32) can be written as:

$$\dot{\vec{A}}(t) = \mathbf{D}\vec{A}(t) + \vec{D} \tag{4.41}$$

where

$$\vec{A}(t) = \begin{pmatrix} \alpha(t) \\ \beta(t) \\ \eta(t) \\ \zeta(t) \end{pmatrix}, \tag{4.42}$$

and

$$\mathbf{D} = \begin{pmatrix} -\kappa - \mathrm{i}\Delta\omega & g & 0 & 0 \\ -g & -\frac{\gamma}{2} - \mathrm{i}\Delta\omega & 0 & 0 \\ \sqrt{2}\mathscr{E} & 0 & -2\kappa - 2\mathrm{i}\Delta\omega & \sqrt{2}g \\ 0 & \mathscr{E} & -\sqrt{2}g & -\left(\kappa + \frac{\gamma}{2}\right) - 2\mathrm{i}\Delta\omega \end{pmatrix}, \tag{4.43a}$$

$$\vec{D} = \begin{pmatrix} \mathscr{E} \\ 0 \\ 0 \\ 0 \end{pmatrix}. \tag{4.43b}$$

To find the steady state of the system, we set the left-hand side of Eq. (4.41) to zero and solve for the state amplitudes, giving

$$\vec{A}_{\mathrm{ss}} = -\mathbf{D}^{-1}\vec{D}. \tag{4.44}$$

To find a general solution of Eq. (4.41), we make a transformation which diagonalises **D**. If **S** is the matrix whose columns are the eigenvalues of **D**, then $\mathbf{\Lambda} \equiv \mathbf{S}^{-1}\mathbf{D}\mathbf{S}$ is the matrix which has the eigenvalues of **D** on the diagonal. With these definitions, Eq. (4.41) becomes

$$\frac{\mathrm{d}}{\mathrm{d}t}\left(\mathbf{S}^{-1}\vec{A}\right) = \mathbf{\Lambda}\left(\mathbf{S}^{-1}\vec{A}\right) + \mathbf{S}^{-1}\vec{D} = \mathbf{\Lambda}\mathbf{S}^{-1}\left(\vec{A} - \vec{A}_{\mathrm{ss}}\right), \tag{4.45}$$

which is integrated to obtain

$$\vec{A}(t) = \mathbf{S}e^{\mathbf{\Lambda}t}\mathbf{S}^{-1}\left[\vec{A}(0) - \vec{A}_{\mathrm{ss}}\right] + \vec{A}_{\mathrm{ss}}. \tag{4.46}$$

For non-zero detuning $\Delta\omega$, inverting **D** or finding its eigenvectors for the general case produces a big mess, which yields little physical insight. For zero detuning there exists a simple solution which can be found in [8, 15]. Instead of finding a full analytic solution, we use a computer to find the steady state $\vec{A}_{\mathrm{ss}}$ by inverting **D**, and to perform the eigenvalue decomposition required for Eq. (4.46). Results are shown in Figs. 4.2 and 4.3.

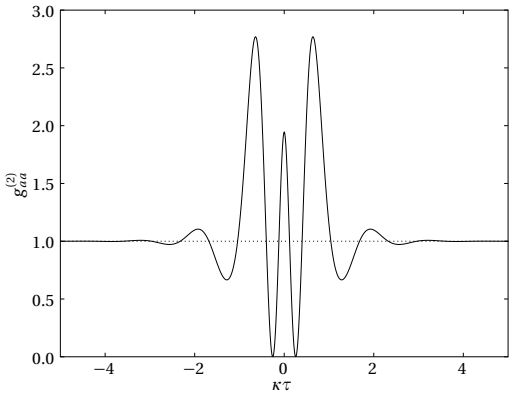

(a) $g^{(2)}_{aa}$ with $g/\kappa = 5$, $\gamma/\kappa = 6$, $\Delta\omega = 0$

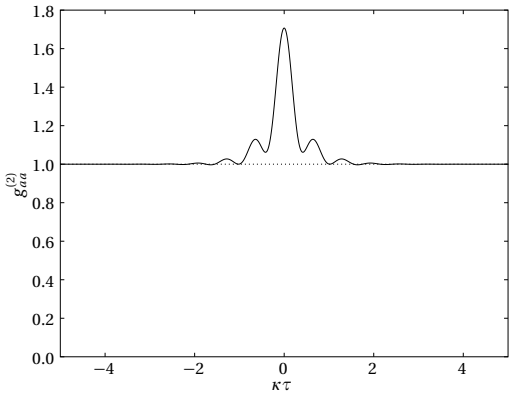

(b) $g^{(2)}_{aa}$ with $g/\kappa = 5$, $\gamma/\kappa = 6$, $\Delta\omega = g$

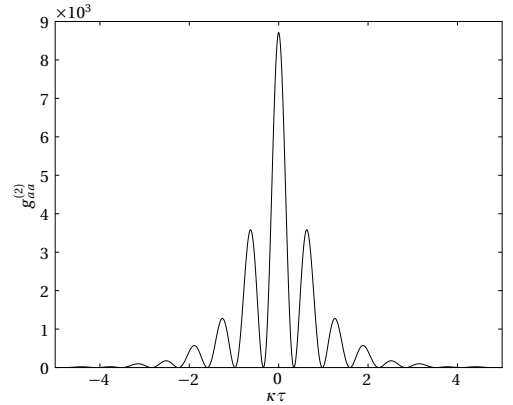

(c) $g^{(2)}_{aa}$ with $g/\kappa = 5$, $\gamma/\kappa = 1$, $\Delta\omega = 0$

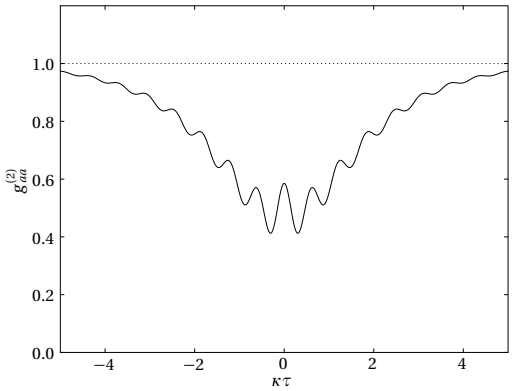

(d) $g^{(2)}_{aa}$ with $g/\kappa = 5$, $\gamma/\kappa = 1$, $\Delta\omega = g$

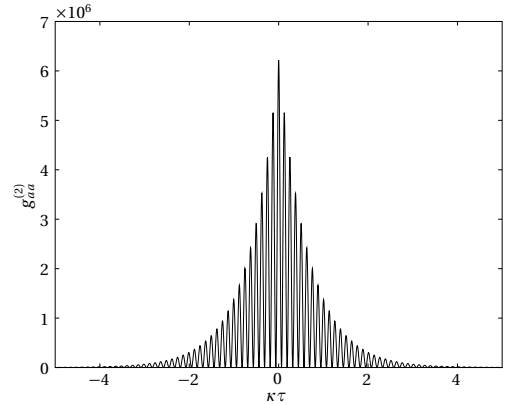

(e) $g^{(2)}_{aa}$ with $g/\kappa = 25$, $\gamma/\kappa = 1$, $\Delta\omega = 0$

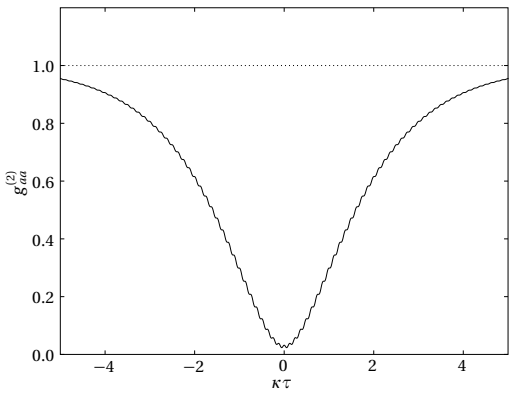

(f) $g^{(2)}_{aa}$ with $g/\kappa = 25$, $\gamma/\kappa = 1$, $\Delta\omega = g$

Figure 4.2: Analytic second-order photon correlation functions, for several values of g/κ and γ/κ, with $\mathscr{E}/\kappa = 0.1$. Examples with no detuning and with $\Delta\omega = g$ are shown. The dotted lines represent the correlation function for coherent light.

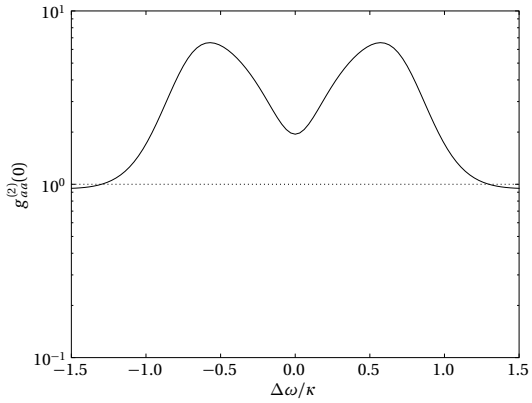

(a) $g^{(2)}_{aa}(0)$ vs. $\Delta\omega/g$, $g/\kappa = 5, \gamma/\kappa = 6$

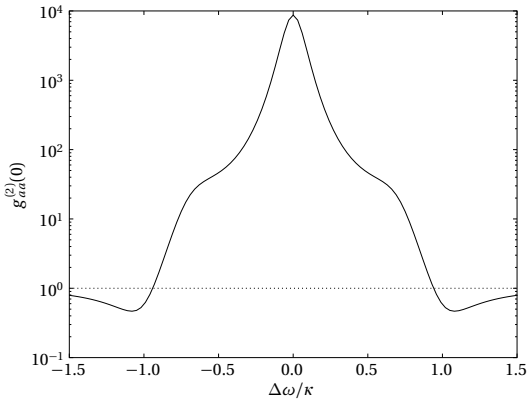

(b) $g^{(2)}_{aa}(0)$ vs. $\Delta\omega/g$, $g/\kappa = 5, \gamma/\kappa = 1$

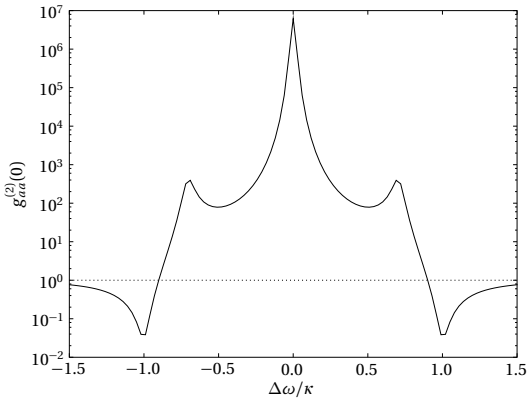

(c) $g^{(2)}_{aa}(0)$ vs. $\Delta\omega/g$, $g/\kappa = 25, \gamma/\kappa = 1$

Figure 4.3: Analytic second-order photon correlation functions at zero time delay plotted against $\Delta\omega/g$, for several values of g/κ and γ/κ, with $\mathscr{E}/\kappa = 0.1$. The dotted lines represent poissonian statistics.

Chapter 5

Numerical solution of the master equation

The master equation is difficult or impossible to solve analytically. Thus numerical solutions of the master equation are necessary to model the behaviour of the system.

5.1 Dimensionless master equation

The floating point numbers in computers have a mantissa of limited precision. This inevitably leads to rounding errors, particularly in the case when adding two non-zero numbers of greatly differing magnitude. There exist arbitrary-precision languages which could in principle solve this problem, but their performance can be inadequate in comparison with computations done in hardware. To avoid this problem, we recast the master equation such that all its terms are of a similar order of magnitude. A dimensionless master equation which satisfies such conditions is a version of Eq. (3.30) scaled by $1/\kappa$ where κ as before is the cavity mode decay rate:

$$\frac{\partial\hat{\rho}}{\partial(\kappa t)} = \left[\frac{\hat{H}_S}{\mathrm{i}\hbar\kappa}, \hat{\rho}\right] + \frac{1}{\kappa}\sum_k \left(\hat{C}_k\hat{\rho}\hat{C}_k^\dagger - \frac{1}{2}\hat{C}_k^\dagger\hat{C}_k\hat{\rho} - \frac{1}{2}\hat{\rho}\hat{C}_k^\dagger\hat{C}_k\right). \tag{5.1}$$

For the collapse operators defined in Eqs. (3.33) and (3.34) the master equation is given by:

$$\begin{aligned}\frac{\partial\hat{\rho}}{\partial(\kappa t)} = \frac{\mathscr{L}}{\kappa}\hat{\rho} = \left[\frac{\hat{H}_S}{\mathrm{i}\hbar\kappa}, \hat{\rho}\right] + 2\left(\hat{a}\hat{\rho}\hat{a}^\dagger - \frac{1}{2}\hat{a}^\dagger\hat{a}\hat{\rho} - \frac{1}{2}\hat{\rho}\hat{a}^\dagger\hat{a}\right) + 2\left(\hat{b}\hat{\rho}\hat{b}^\dagger - \frac{1}{2}\hat{b}^\dagger\hat{b}\hat{\rho} - \frac{1}{2}\hat{\rho}\hat{b}^\dagger\hat{b}\right) \\ + \frac{\gamma}{\kappa}\sum_{n=-1,0,1}\left(\hat{\Sigma}_n\hat{\rho}\hat{\Sigma}_n^\dagger - \frac{1}{2}\hat{\Sigma}_n^\dagger\hat{\Sigma}_n\hat{\rho} - \frac{1}{2}\hat{\rho}\hat{\Sigma}_n^\dagger\hat{\Sigma}_n\right)\end{aligned} \tag{5.2}$$

with

$$\begin{aligned}\frac{\hat{H}_S}{\mathrm{i}\hbar\kappa} = \frac{\mathscr{E}}{\kappa}\left(\hat{a}^\dagger - \hat{a}\right) - \mathrm{i}\frac{\Delta\omega}{\kappa}\left(\hat{a}^\dagger\hat{a} + \hat{b}^\dagger\hat{b}\right) - \mathrm{i}\sum_{m_F=-4}^{4}\left(-\frac{1}{2}\frac{\Delta\omega}{\kappa} + g_{F,g}m_F\frac{\mathscr{B}}{\kappa}\right)|g,m_F\rangle\langle g,m_F| \\ - \mathrm{i}\sum_{m_F=-5}^{5}\left(+\frac{1}{2}\frac{\Delta\omega}{\kappa} + g_{F,e}m_F\frac{\mathscr{B}}{\kappa}\right)|e,m_F\rangle\langle e,m_F| \\ - \frac{g}{\kappa}\left(\hat{a}\hat{\Sigma}_0^\dagger - \hat{a}^\dagger\hat{\Sigma}_0\right) - \frac{g}{\kappa}\left(\hat{b}\left[\frac{\hat{\Sigma}_{-1}^\dagger + \hat{\Sigma}_{+1}^\dagger}{\sqrt{2}}\right] - \hat{b}^\dagger\left[\frac{\hat{\Sigma}_{-1} + \hat{\Sigma}_{+1}}{\sqrt{2}}\right]\right)\end{aligned} \tag{5.3}$$

where $\Delta\omega = \omega_0 - \omega_L$ is the detuning of the laser frequency from resonance and $\mathscr{B} = \mu_B B/\hbar$. For the experiment we are modelling, $\Delta\omega = g$.

We have five dimensionless parameters that can be varied to investigate the dynamics of the system: γ/κ, $\mathscr{E}/\kappa$, $\mathscr{B}/\kappa$, $\Delta\omega/\kappa$ and g/κ.

5.2 Steady state properties

The steady state of the system is of course defined by the condition

$$\dot{\rho}(\infty) = \mathscr{L}\rho(\infty) = 0 \tag{5.4}$$

where $\rho(\infty)$ is the steady state reduced density operator or density matrix of the system, and $\mathscr{L}$ is the Liouvillian, defined in Eq. (3.32). If the density operator is written as a vector in which each element corresponds to an element of the $n \times n$ square density matrix, then the Liouvillian superoperator can be written as a square $n^2 \times n^2$ matrix. Finding the nullspace of the Liouvillian matrix yields the solution to the steady state equation, Eq. (5.4).

Once we know the steady state density operator of the system, $\rho(\infty)$, we are able to calculate expectation values of operators in the steady state using Eq. (3.3).

Therefore we can easily calculate the mean photon numbers of the driven and non-driven modes in the steady state:

$$\langle \hat{N}_a \rangle_{\mathrm{ss}} = \langle \hat{a}^\dagger \hat{a} \rangle_{\mathrm{ss}} = \mathrm{tr}\left[\hat{a}^\dagger \hat{a}\, \rho(\infty)\right], \tag{5.5a}$$

$$\langle \hat{N}_b \rangle_{\mathrm{ss}} = \langle \hat{b}^\dagger \hat{b} \rangle_{\mathrm{ss}} = \mathrm{tr}\left[\hat{b}^\dagger \hat{b}\, \rho(\infty)\right]. \tag{5.5b}$$

Using the quantum regression formula in Eq. (3.45), it is possible to also evaluate the steady state second-order photon correlation function defined in Eq. (1.4):

$$g^{(2)}_{\mu\nu}(\tau) = \frac{\langle \hat{\mu}^\dagger(0)\hat{\nu}^\dagger(\tau)\hat{\nu}(\tau)\hat{\mu}(0)\rangle_{\mathrm{ss}}}{\langle \hat{\mu}^\dagger\hat{\mu}\rangle_{\mathrm{ss}}\langle \hat{\nu}^\dagger\hat{\nu}\rangle_{\mathrm{ss}}} = \frac{1}{\langle \hat{\nu}^\dagger\hat{\nu}\rangle_{\mathrm{ss}}}\mathrm{tr}\left[\hat{\nu}^\dagger\hat{\nu}\, \exp\{\mathscr{L}\tau\}\left(\frac{\hat{\mu}\rho(\infty)\hat{\mu}^\dagger}{\langle \hat{\mu}^\dagger\hat{\mu}\rangle_{\mathrm{ss}}}\right)\right]. \tag{5.6}$$

For numerical reasons, the collapsed density matrix $\hat{\mu}\rho(\infty)\hat{\mu}^\dagger$ is normalised by $\langle \hat{\mu}^\dagger\hat{\mu}\rangle_{\mathrm{ss}}$ in order that the matrix elements do not become too small during computation.

If we define

$$\varrho(\tau) = \exp\{\mathscr{L}\tau\}\left(\frac{\hat{\mu}\rho(\infty)\hat{\mu}^\dagger}{\langle \hat{\mu}^\dagger\hat{\mu}\rangle_{\mathrm{ss}}}\right) \tag{5.7}$$

it is clear that

$$\varrho(0) = \frac{\hat{\mu}\rho(\infty)\hat{\mu}^\dagger}{\langle \hat{\mu}^\dagger\hat{\mu}\rangle_{\mathrm{ss}}} \tag{5.8}$$

and

$$\frac{\mathrm{d}}{\mathrm{d}\tau}\varrho(\tau) = \mathscr{L}\exp\{\mathscr{L}\tau\}\left(\frac{\hat{\mu}\rho(\infty)\hat{\mu}^\dagger}{\langle \hat{\mu}^\dagger\hat{\mu}\rangle_{\mathrm{ss}}}\right) = \mathscr{L}\varrho(\tau), \tag{5.9}$$

or equivalently,

$$\frac{\mathrm{d}}{\mathrm{d}(\kappa\tau)}\varrho = \frac{\mathscr{L}}{\kappa}\varrho. \tag{5.10}$$

Thus, we have a first-order differential equation for $\varrho(\tau)$ with an initial condition. This can be used to avoid computationally expensive matrix exponentiation operations in the calculation of the steady state second-order photon correlation function. The second-order photon correlation function is given by

$$g^{(2)}_{\mu\nu}(\tau) = \frac{1}{\langle \hat{\nu}^\dagger\hat{\nu}\rangle_{\mathrm{ss}}}\mathrm{tr}\left[\hat{\nu}^\dagger\hat{\nu}\,\varrho(\tau)\right]. \tag{5.11}$$

5.3 Fock space truncation

For appropriately chosen combinations of parameters, the number of photons in a given cavity mode α is unlikely to exceed a maximum number, N_α. Therefore it is clearly a good approximation to neglect all Fock states with a photon number larger than N_α. This is referred to as truncating the Fock space of the cavity mode α.

If, in our calculation, N_a and N_b are respectively the maximum allowed photon numbers in the driven and non-driven cavity modes, and N_{atom} is the number of atomic states considered, the Hilbert space $\mathscr{H}$ of the atom-cavity system,

$$\mathscr{H} = \mathscr{H}_{\text{atom}} \otimes \mathscr{H}_a \otimes \mathscr{H}_b, \tag{5.12}$$

will be $N_{\text{atom}}(N_a+1)(N_b+1)$-dimensional. To solve a master equation of this dimensionality requires the solution of a set of $[N_{\text{atom}}(N_a+1)(N_b+1)]^2$ coupled differential equations. For large N_a and N_b this task can become too difficult numerically to be worth pursuing. It is sensible, then, to choose small enough N_a and N_b that the solution of the master equation will be straightforward, but not so small that the results are unduly affected.

5.4 Numerical modelling

The numerical solutions of the master equation presented in the following sections were computed using programs written in the PYTHON programming language [3]. Much use was made of the Python-compatible packages NUMPY [2] and SCIPY [4]: the former contains subroutines and data structures for scientific computing and linear algebra; the latter contains further useful packages, in particular sparse matrix structures and numerical integration routines. Plots and graphics were produced using MATPLOTLIB [1].

5.5 Driven two-level atom in an optical cavity

The system consisting of a driven two-level atom in an optical cavity has Hamiltonian

$$\frac{\hat{H}}{\mathrm{i}\hbar\kappa} = \frac{\mathscr{E}}{\kappa}\left(\hat{a}^\dagger - \hat{a}\right) - \mathrm{i}\frac{\Delta\omega}{\kappa}\hat{a}^\dagger\hat{a} - \mathrm{i}\frac{1}{2}\frac{\Delta\omega}{\kappa}\hat{\sigma}_z - \frac{g}{\kappa}\left(\hat{a}\hat{\sigma}_+ - \hat{a}^\dagger\hat{\sigma}_-\right) \tag{5.13}$$

with $\hat{\sigma}_z$ as defined in Eq. (2.8). The master equation is given by Eq. (3.30) with collapse operators for the cavity modes given by Eqs. (3.33), and atomic collapse operator given by

$$\hat{C}_{\text{atom}} = \sqrt{\gamma}\hat{\sigma}_-. \tag{5.14}$$

The mean photon number can be calculated according to Eq. (5.5a), while the mean occupation of the atomic excited state is given by

$$\langle\hat{\sigma}_+\hat{\sigma}_-\rangle_{\text{ss}} = \text{tr}\left[\hat{\sigma}_+\hat{\sigma}_-\rho(\infty)\right]. \tag{5.15}$$

These averages are calculated in [19] using a quantum trajectory method, and identical results obtained using the master equation technique are shown in Fig. 5.1.

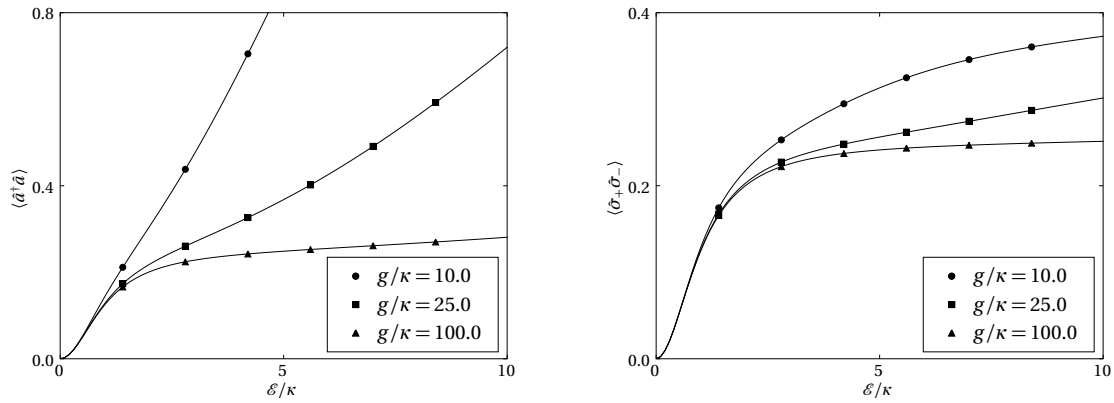

(a) $\langle \hat{a}^\dagger \hat{a} \rangle$ vs. $\mathscr{E}/\kappa$

(b) $\langle \hat{\sigma}_+ \hat{\sigma}_- \rangle$ vs. $\mathscr{E}/\kappa$

Figure 5.1: Steady state properties of a driven two-level atom in an optical cavity with $\gamma/\kappa = 2$ and $\Delta\omega = g$, for several values of g/κ. These results were obtained with a basis truncated at the six-photon level.

5.6 Results for a driven two-level atom in an optical cavity with Zeeman substructure

We now take into account the full atomic level structure for an $F = 4 \longleftrightarrow F' = 5$ transition, in which case the master equation and Hamiltonian are given by Eqs. (5.2) and (5.3).

For an $F = 4 \longleftrightarrow F' = 5$ transition, there are nine magnetic sublevels of the ground state, and eleven magnetic sublevels of the excited state, giving a total of twenty atomic states that must be considered. Consequently, it is necessary to truncate the Fock spaces of the driven and non-driven cavity modes at a comparatively low level, to reduce the number of coupled differential equations that must be solved, and avoid computational difficulties. All the results presented in this section were obtained with the basis for driven mode truncated at the two-photon level, and the basis for the non-driven mode truncated at the one-photon level. That is to say, $N_a = \{0,1,2\}$ and $N_b = \{0,1\}$. Such low photon numbers mean that this method can only be used to find valid results in the weak excitation regime.

The quantities of interest are the second-order photon correlation functions, which allow us to identify the non-classical properties of light: sub-poissonian photon statistics and photon anti-bunching. The quantum regression formula, as given in Eq. (5.6), is used to calculate the correlation functions. The self-correlation for the driven mode is symmetrical about zero:

$$g^{(2)}_{aa}(-\tau) \equiv g^{(2)}_{aa}(\tau), \tag{5.16}$$

by definition. The two-mode cross-correlation $g^{(2)}_{ba}$ is not symmetrical. $g^{(2)}_{ba}(\tau)$ relates to the arrival at the detector of a photon in the non-driven mode b at time zero, and of a photon in the driven mode a at time τ. $g^{(2)}_{ba}(-\tau)$, on the other hand, relates to the arrival of a photon in the driven mode at time zero, and the non-driven mode at time τ. Thus,

$$g^{(2)}_{ba}(-\tau) \equiv g^{(2)}_{ab}(\tau). \tag{5.17}$$

5.6.1 Resonant driving field

We now solve the master equation for a driven two-level atom in an optical cavity, with the driving field resonant with the cavity: $\Delta\omega = 0$. The full atomic level structure is taken into account; however

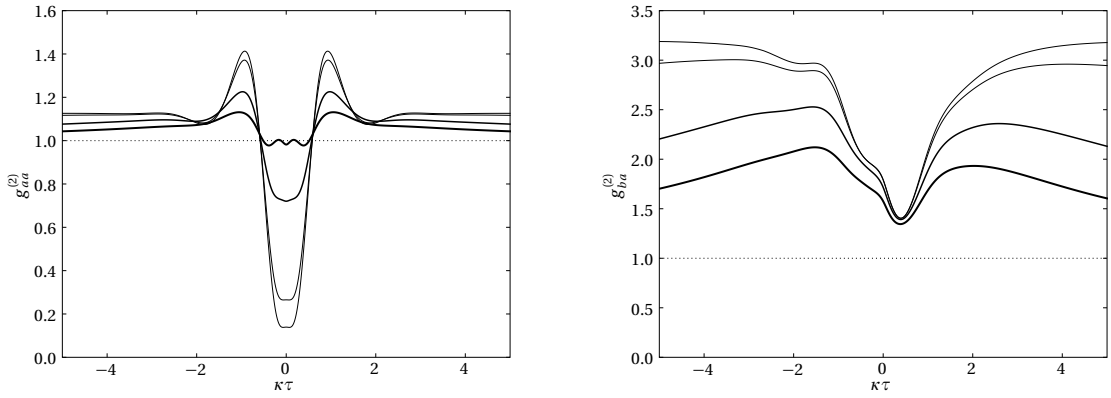

(a) Driven mode self-correlation, $g^{(2)}_{aa}$

(b) Two-mode cross-correlation, $g^{(2)}_{ba}$

Figure 5.2: Steady state photon correlation functions for an $F = 4 \longleftrightarrow F' = 5$ transition, with $\gamma/\kappa = 6$, $g/\kappa = 5$, $\Delta\omega/\kappa = 0$, and $\mathscr{E}/\kappa = 0.1, 0.3, 0.7$, and 1.0, from thinnest line to thickest. The dotted lines represent the correlation function for coherent light.

the external magnetic field which defines the quantisation axis is assumed to be negligible. Self-correlations and cross-correlations are plotted in Fig. 5.2.

5.6.2 Effect of detuning

In the weak excitation regime, changing the detuning of the driving laser from the cavity has a substantial effect on the form of the second-order photon correlation functions. Self-correlations and cross-correlations for several detunings, ranging from $\Delta\omega = 0$ to $\Delta\omega = g$, are shown in Fig. 5.3, as are correlation functions at zero time delay as a function of detuning, with similar parameters.

Note that for the parameters examined, increasing the detuning can cause a transition from sub-poissonian to super-poissonian photon statistics, or vice versa. As the experiment being modelled has $\Delta\omega = g$, it will be necessary to find a set of parameters which allow sub-poissonian photon statistics to be observed.

Photon correlation functions for the case where $\Delta\omega = g$ are shown in Fig. 5.4 for several driving field strengths and two different values of g/κ.

5.6.3 Effect of external magnetic field

We now consider the case of non-negligible external magnetic field. In the case where no external magnetic field is applied, all the magnetic sublevels of the atomic $F = 4$ ground state are degenerate, as are those of the $F' = 5$ excited state. Each of the dressed states will be split into a manifold of magnetic sublevels, even when the magnetic field is taken to be have negligible Zeeman effect, because of the different Clebsch-Gordan coefficients appearing in Eqs. (2.42). In effect, there are different coupling strengths to the cavity mode depending on which magnetic sublevel the atom is in. The Zeeman effect introduces an additional energy shift, altering the spacing of the sublevels within each manifold. What effect the coupling to the non-driven mode (which is not present in the simple Jaynes-Cummings model) will have on the energy level structure is not clear at this stage, and could be investigated further.

In Fig. 5.5, self-correlations and cross-correlations are plotted for several strengths of the external magnetic field, with other parameters held constant. In Fig. 5.6, correlation functions are shown with several driving field strengths, for two different magnetic field strengths.

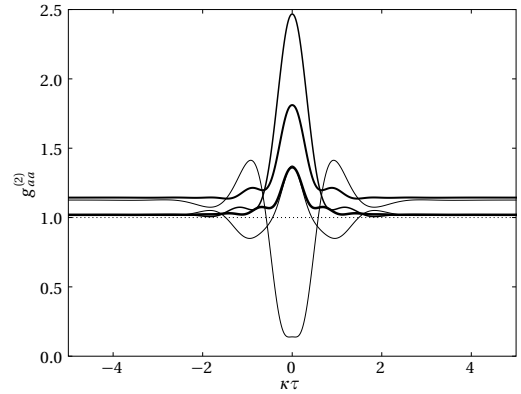

(a) Driven mode self-correlation, $g^{(2)}_{aa}$

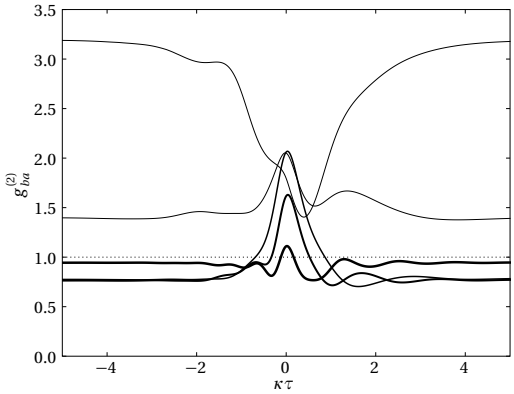

(b) Two-mode cross-correlation, $g^{(2)}_{ba}$

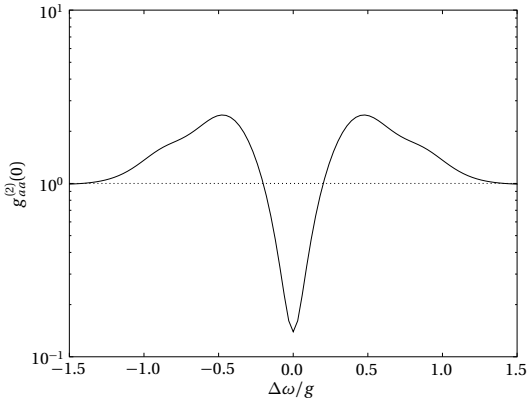

(c) $g^{(2)}_{aa}(0)$ vs. $\Delta\omega/g$, $\gamma/\kappa = 6$, $g/\kappa = 5$

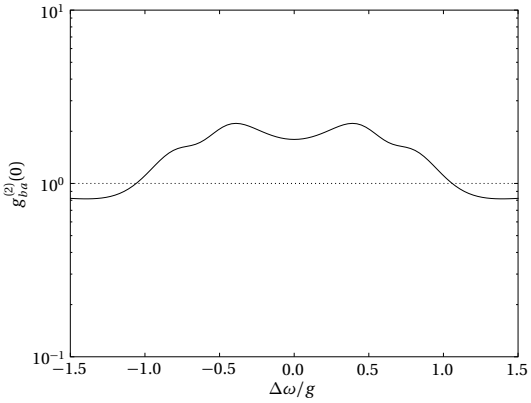

(d) $g^{(2)}_{ba}(0)$ vs. $\Delta\omega/g$, $\gamma/\kappa = 6$, $g/\kappa = 5$

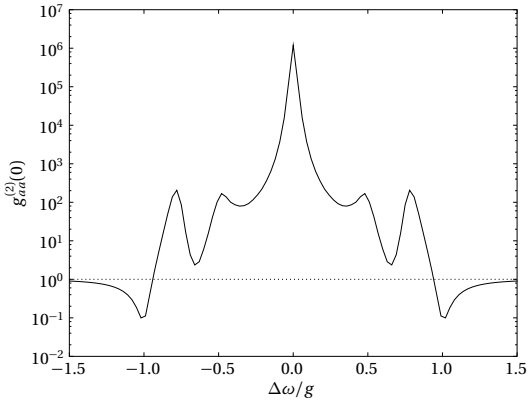

(e) $g^{(2)}_{aa}(0)$ vs. $\Delta\omega/g$, $\gamma/\kappa = 1$, $g/\kappa = 25$

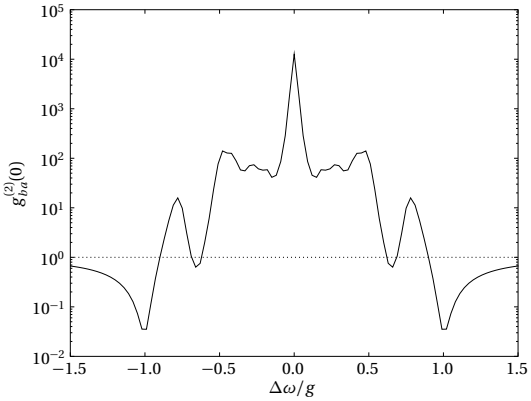

(f) $g^{(2)}_{ba}(0)$ vs. $\Delta\omega/g$, $\gamma/\kappa = 1$, $g/\kappa = 25$

Figure 5.3: Steady state photon correlation functions for an $F = 4 \longleftrightarrow F' = 5$ transition. The driven mode self-correlation is shown in (a) and the two-mode cross correlation in (b), with $\gamma/\kappa = 6$, $g/\kappa = 5$, $\mathscr{E}/\kappa = 0.1$ and $\Delta\omega/\kappa = 0$, 1.25, 2.5, 3.75, and 5, from thinnest line to thickest. The self-correlation and cross-correlation at zero time delay are shown in (c) & (e) and (d) & (f) respectively, as a function of detuning, with $\mathscr{E}/\kappa = 0.1$. Parameters for (c) and (d) are $\gamma/\kappa = 6$ and $g/\kappa = 5$; (e) and (f) have $\gamma/\kappa = 1$ and $g/\kappa = 25$. The dotted lines represent the correlation function for coherent light in (a) & (b) and poissonian statistics in (c), (d), (e) & (f).

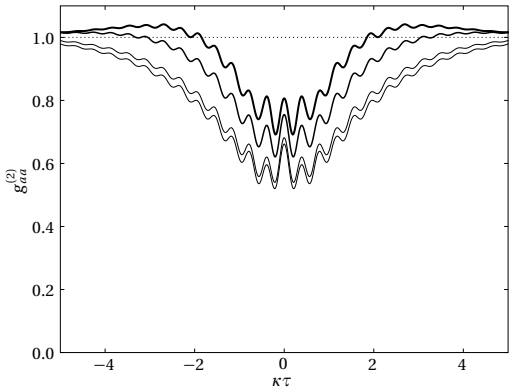

(a) Driven mode self-correlation, $g^{(2)}_{aa}$, $g/\kappa = 8$

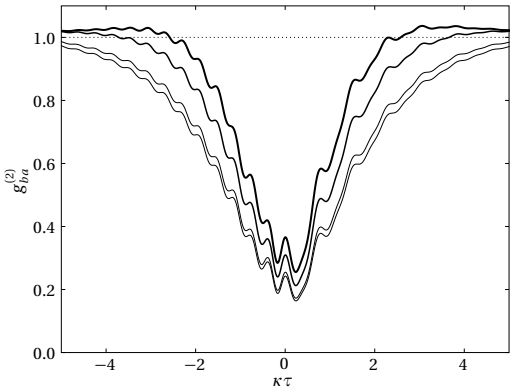

(b) Two-mode cross-correlation, $g^{(2)}_{ba}$, $g/\kappa = 8$

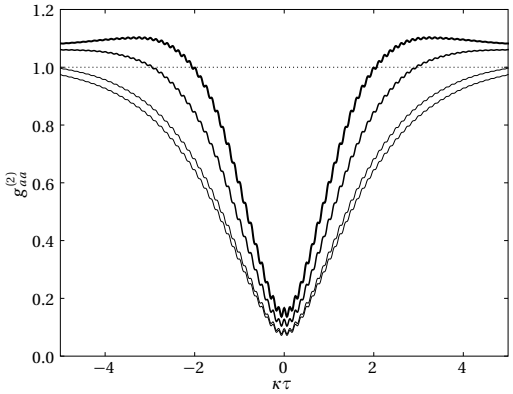

(c) Driven mode self-correlation, $g^{(2)}_{aa}$, $g/\kappa = 25$

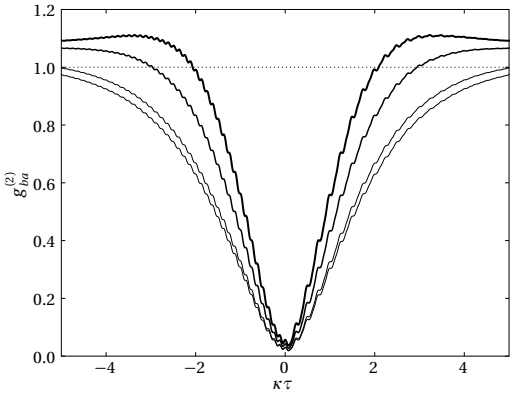

(d) Two-mode cross-correlation, $g^{(2)}_{ba}$, $g/\kappa = 25$

Figure 5.4: Steady state photon correlation functions for an $F = 4 \longleftrightarrow F' = 5$ transition, with $\gamma/\kappa = 1$, $\Delta\omega/\kappa = g/\kappa$, and $\mathscr{E}/\kappa = 0.1$, 0.3, 0.7, and 1.0, from thinnest line to thickest. Figures (a) and (b) have $g/\kappa = 8$, while (c) and (d) have $g/\kappa = 25$. The dotted lines represent the correlation function for coherent light.

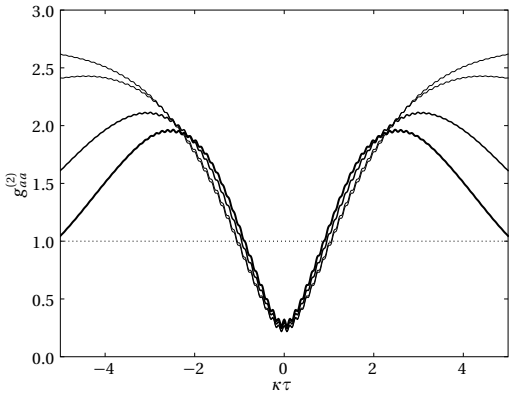

(a) Driven mode self-correlation, $g^{(2)}_{aa}$

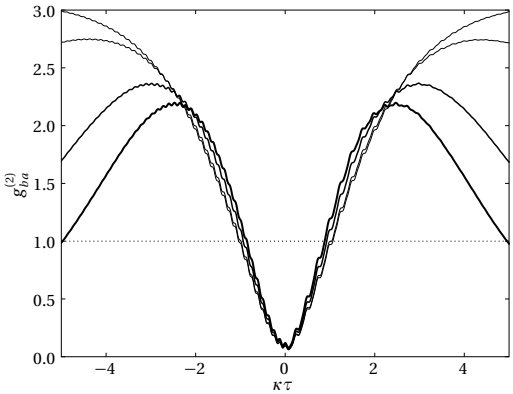

(b) Two-mode cross-correlation, $g^{(2)}_{ba}$

Figure 5.5: Steady state photon correlation functions for an $F = 4 \longleftrightarrow F' = 5$ transition, with $\gamma/\kappa = 1$, $g/\kappa = 25$, $\Delta\omega/\kappa = g/\kappa$, $\mathscr{E}/\kappa = 0.1$ and $\mathscr{B}/\kappa = 0.1$, 0.3, 0.7, and 1.0, from thinnest line to thickest. The dotted lines represent the correlation function for coherent light.

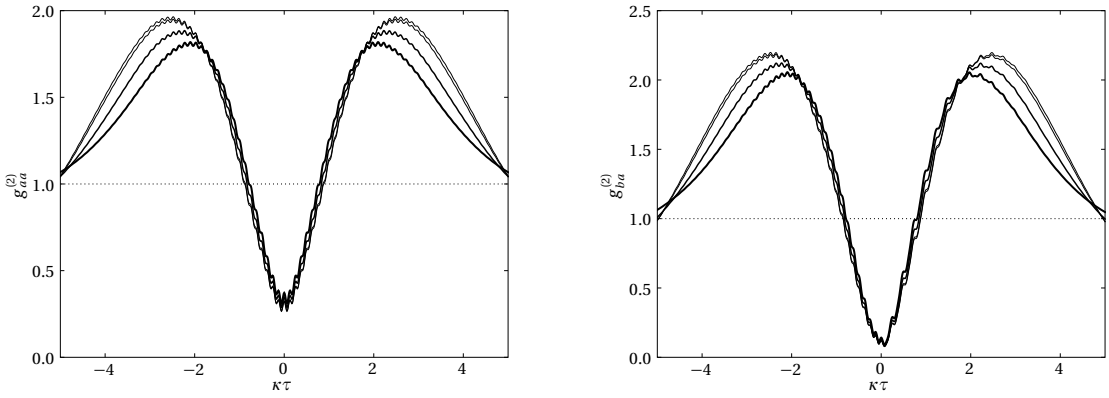

(a) Driven mode self-correlation, $g^{(2)}_{aa}$, $\mathscr{B}/\kappa = 1$

(b) Two-mode cross-correlation, $g^{(2)}_{ba}$, $\mathscr{B}/\kappa = 1$

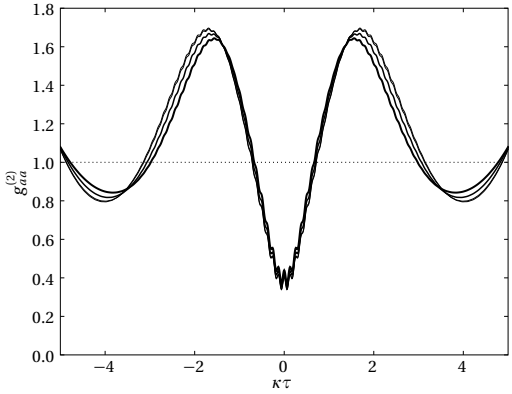

(c) Driven mode self-correlation, $g^{(2)}_{aa}$, $\mathscr{B}/\kappa = 2$

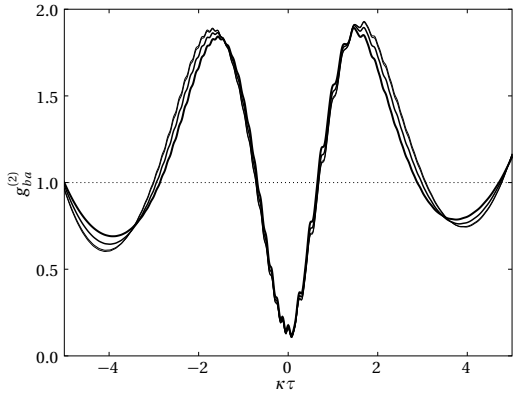

(d) Two-mode cross-correlation, $g^{(2)}_{ba}$, $\mathscr{B}/\kappa = 2$

Figure 5.6: Steady state photon correlation functions for an $F = 4 \longleftrightarrow F' = 5$ transition, with $\gamma/\kappa = 1$, $g/\kappa = 25$, $\Delta\omega/\kappa = g/\kappa$, and $\mathscr{E}/\kappa = 0.1$, 0.3, 0.7, and 1.0, from thinnest line to thickest. Figures (a) and (b) have $\mathscr{B}/\kappa = 1$, while (c) and (d) have $\mathscr{B}/\kappa = 2$. The dotted lines represent the correlation function for coherent light.

5.7 Interpretation of results

5.7.1 Origin of oscillations in second-order photon correlation functions

We observe in the results obtained by numerical solution of the master equation that both driving laser detuning and external magnetic field introduce oscillations into the second-order correlation functions: both the driven mode self-correlation and the two-mode cross-correlation are similarly affected. It is not surprising, from a mathematical perspective, that laser detuning and magnetic field have similar effects: both appear in the atomic Hamiltonian as terms on the main diagonal. The magnetic field is a detuning like the detuning of the laser, in the sense that it shifts the energies of the atom away from resonance with the driving field: the effect of the magnetic field is to lift the degeneracy of the atomic ground and excited states, and to shift the energies of these states.

We can interpret the oscillations due to the laser detuning in the context of the analytic investigations into the Jaynes-Cummings model developed in §4.2. Non-zero laser detuning introduces complex terms into the equations of motion of the state amplitudes (4.32). Thus, detuning naturally results in damped oscillations of the complex amplitudes of the two dressed states on the first rung of the Jaynes-Cummings ladder (Fig. 4.1). Equation (4.40) relates the second-order photon correlation

function to the square modulus of the amplitude of the state $|g\rangle|1\rangle$ (see Eqs. (4.31) and (4.36)); as such, oscillations in the state amplitudes will correspond to oscillations in the second-order photon correlation functions.

In the case of the more complicated level structure, for which numerical solutions have been obtained in Chapter 5, we are considering not the dressed states of the Jaynes-Cummings ladder but the manifolds of energy-shifted states which correspond to the dressed states. All the same, the analysis in terms of the oscillations in the amplitudes of the dressed states conveys the essential physics.

The effect of applying an external magnetic field to the system is to cause the magnetic moment of the electron to precess about the magnetic field; this is what causes the Zeeman effect. This Larmor precession (see Appendix E of [13] for an overview) manifests itself as low-frequency oscillations in the second-order correlation function, determined by the Larmor frequency.

5.7.2 Non-classical properties of light

We remind ourselves of the two distinctly quantum phenomena which we are interested in identifying. The first is the appearance of sub-poissonian photon statistics, identified by the condition

$$g^{(2)}(0) < 1. \tag{5.18}$$

The second quantum phenomenon is photon antibunching, identified by the condition

$$g^{(2)}(\tau) > g^{(2)}(0), \quad \forall\ \tau. \tag{5.19}$$

As was mentioned in §1.3.2, sub-poissonian photon statistics and photon antibunching can potentially occur together, but each can also occur in the absence of the other.

It is important to consider the relevance of the two-mode cross correlations to the interpretation of the behaviour of the system. Even if the cross-correlation satisfies, mathematically, the inequality for sub-poissonian photon statistics, for photon antibunching, or for both, this is not necessarily an indication of non-classical behaviour. Two classical variables can be anti-correlated in such a way as to produce these phenomena; a quantum system is not necessarily required to produce such behaviour. In fact, the definitions of sub-poissonian photon statistics and photon antibunching hold for the self-correlation but not for the cross-correlation. As such, in this section we will only consider the results obtained for the self-correlation.

We have identified parameter regimes for which sub-poissonian photon statistics are apparent. This is perhaps shown most clearly in Figs. 5.3(c) and 5.3(e), in which we have plotted the driven mode self-correlation $g^{(2)}_{aa}$ against the ratio $\Delta\omega/g$ (the detuning in units of the atom-cavity coupling constant). Both figures show that there exist parameters for which the photon statistics of the light, as characterised by the second-order correlation functions, are sub-poissonian.

We can see that in Fig. 5.2(a), where the driving laser is resonant with the cavity mode, the driven mode self-correlation satisfies the condition for photon antibunching. However, when laser detuning is introduced (see Fig. 5.4) is it more difficult to find parameter regimes which unambiguously display photon antibunching. While it is simple enough to tweak the values of g/κ and γ/κ so that the photon statistics are sub-poissonian when, for example, $\Delta\omega = g$, the oscillations which the detuning introduces can prevent the correlation function $g^{(2)}_{aa}$ from having a global minimum at $\tau = 0$, as is required for photon antibunching.

It is important to note, however, that for classical light, the second-order correlation function always has a global maximum at $\tau = 0$, and tends to unity as $\tau \to \infty$. Thus any second-order correlation function which starts below unity is, despite the fact that it may not technically exhibit photon antibunching, an indication of distinctly quantum phenomena that cannot be explained classically.

Chapter 6

Conclusion

6.1 Summary

In this dissertation, we have computed second-order photon correlation functions in a system where two optical cavity modes with orthogonal linear polarisations interact with an atom via an $F = 4 \longleftrightarrow F' = 5$ transition. We took into account the full atomic level structure for this transition, including the Zeeman splitting of the magnetic sublevels. One cavity mode couples the $F = 4$ atomic state to the $F' = 5$ state via $\Delta m_F = 0$ transitions; the other cavity mode couples the atomic states via $\Delta m_F = \pm 1$ transitions. The former mode is driven by a coherent laser field.

We investigated analytically a comparatively simple system consisting of a two-level atom in a single-mode cavity, for the case of a weak driving field. Steady state correlation functions were thus obtained using standard quantum regression formulae.

We used a numerical solution of the master equation for the system in the steady state to obtain second-order photon correlation functions for the more complicated system, taking into account the full atomic level structure and the second cavity mode. These numerical solutions were obtained in the weak excitation regime and thus we were able to truncate the cavity mode Hilbert spaces at the two-photon and one-photon levels for the driven and non-driven modes respectively, making the numerical computations tractable.

We interpreted the results of the numerical solutions of the master equation, noting that energy shifts — whether due to the laser detuning, or due to the Zeeman effect produced by an external magnetic field — cause oscillations in time to appear in the steady-state second-order photon correlation functions.

We can draw from the second-order correlation functions the conclusion that non-classical phenomena are present in the system being modelled. The photon statistics of our system, characterised by the second-order photon correlation function, were sub-poissonian for several of the parameter regimes for which results were obtained. Whether or not photon antibunching was observed is less clear; it is certain, however, that the photon correlation functions indicated distinctly quantum phenomena.

6.2 Future work

The treatment presented in this dissertation is limited to the weak-excitation regime by computational concerns. For higher driving field strengths, larger numbers of photons may be present in both cavity modes. As such, the dimensionality of the system Hilbert space becomes large enough that solving the master equation becomes impractical. In [15], a Monte-Carlo simulation is used to

take into account higher excitations of the cavity modes, without introducing the kind of computational difficulty which limits the master equation approach. A possible future project would be to implement a Monte-Carlo simulation of the model developed in this dissertation.

Modifications to the model developed in this dissertation are possible. The model may, for example, in future be extended by taking into account the birefringence of the cavity mirrors, thereby coupling the two cavity modes even when there is no atom present in the cavity.

In a real-world experiment, atoms do not remain stationary in the centre of an optical cavity. Typically, an atomic beam traverses the cavity. As an atom passes through the cavity, it experiences a different atom-cavity coupling strength at different locations. The model could therefore be extended to take into account the varying coupling strength due to the motion of the atom.

It is mentioned above that whether or not photon antibunching was observed in our results is ambiguous. A way of clearing up this ambiguity would be to investigate the *waiting-time distribution* for the photon emission events. The details are beyond the scope of this dissertation; the reader is referred to [19] for more information.

Another area of interest is the effect of the coupling to the non-driven mode on the energy level structure of the atom-cavity system. As mentioned in §5.6.3, working out the explicit level structure for the complete system may be an interesting future project.

Bibliography

[1] *matplotlib*, `matplotlib.sourceforge.net`.

[2] *NumPy*, `numpy.scipy.org`.

[3] *Python programming language*, `python.org`.

[4] *SciPy*, `scipy.org`.

[5] K. M. Birnbaum, A. Boca, R. Miller, A. D. Boozer, T. E. Northup, and H. J. Kimble, *Photon blockade in an optical cavity with one trapped atom*, Nature **436** (2005), 87.

[6] _____, *Theory of photon blockade by an optical cavity with one trapped atom*, unpublished, 2005, `arxiv.org/abs/quant-ph/0507065v1`.

[7] H. J. Carmichael, *Statistical Methods in Quantum Optics*, vol. 1, Springer, 1999.

[8] _____, *Statistical Methods in Quantum Optics*, vol. 2, Springer, 2008.

[9] D. Deutsch, *Quantum theory, the Church-Turing principle and the universal quantum computer*, Proceedings of the Royal Society of London A **400** (1985), 97.

[10] A. R. Edmonds, *Angular Momentum in Quantum Mechanics*, Princeton University Press, 1957.

[11] R. P. Feynman, *Simulating Physics with Computers*, International Journal of Theoretical Physics **21** (1982), no. 6-7, 467.

[12] C. J. Foot, *Atomic Physics*, Oxford University Press, 2006.

[13] A. M. Fox, *Quantum Optics*, Oxford University Press, 2007.

[14] E. T. Jaynes and F. W. Cummings, *Comparison of quantum and semiclassical radiation theories with application to the beam maser*, Proceedings of the IEEE **51** (1963), 89.

[15] Matthias Kronenwett, *Photon Correlations in Two-Mode Cavity Quantum Electrodynamics*, Master's thesis, University of Auckland, 2007.

[16] R. Loudon, *The Quantum Theory of Light*, third ed., Oxford University Press, 2000.

[17] J. J. Sakurai, *Modern Quantum Mechanics*, revised ed., Addison-Wesley, 1994.

[18] P. W. Shor, *Algorithms for Quantum Computation: Discrete Logarithms and Factoring*, Proceedings of the 35$^{\text{th}}$ Annual Symposium on Foundations of Computer Science (1994), 124.

[19] L. Tian and H. J. Carmichael, *Quantum trajectory simulations of the two-state behaviour of an optical cavity containing one atom*, Physical Review A **46** (1992), no. 11, R6801.